

Title: Clusters of Galaxies in Microwave and X-Ray Spectral Bands

Date: Apr 30, 2009 09:45 AM

URL: <http://pirsa.org/09040053>

Abstract:

PERIMETER INSTITUTE

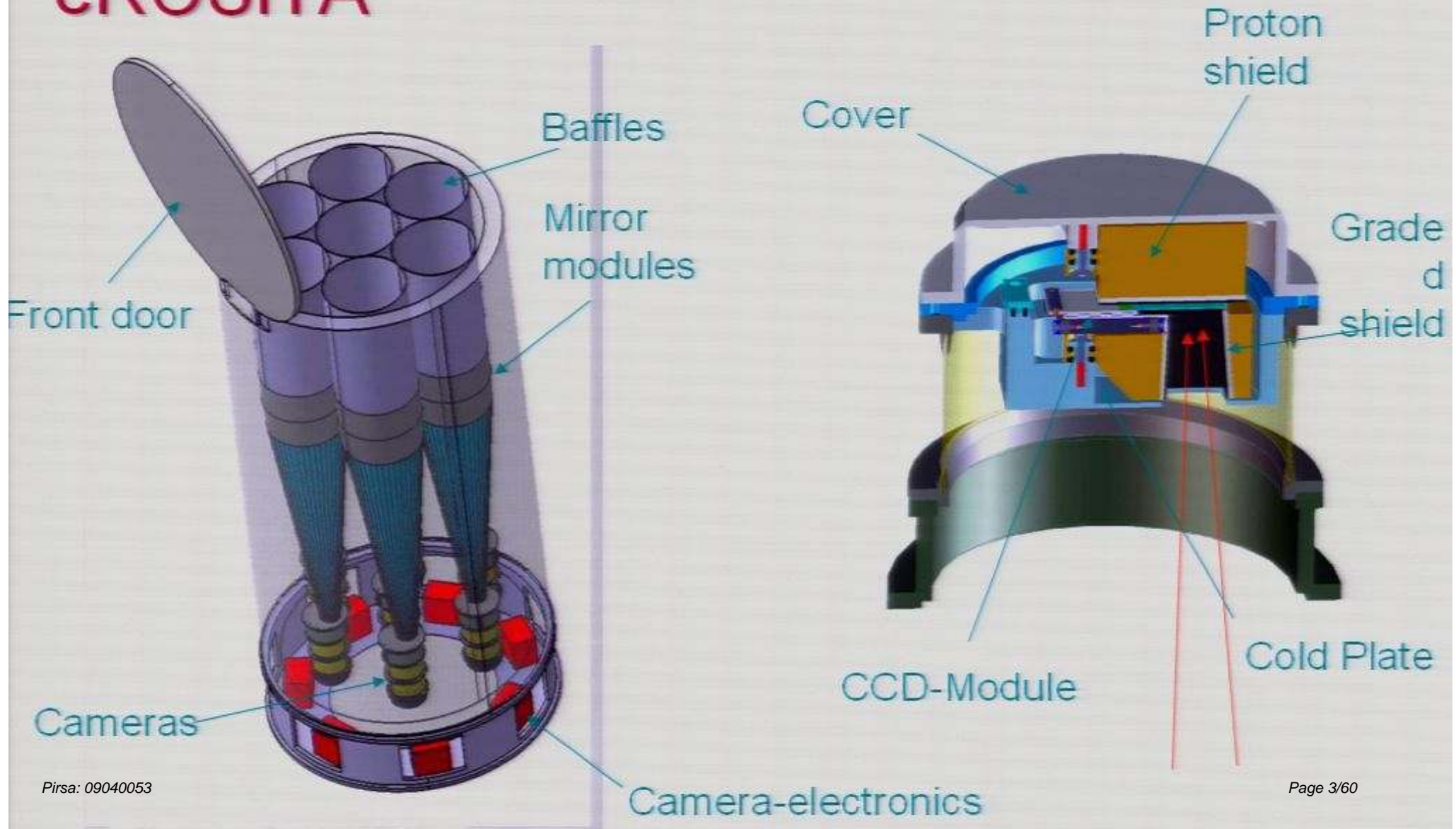
**Clusters of galaxies in Microwave and X-Ray spectral bands**  
*(spectroscopy and polarization)*

**Rashid Sunyaev**



*Max-Planck-Institut für Astrophysik  
and  
Space Research Institute  
of Russian Academy of Sciences*

# eROSITA



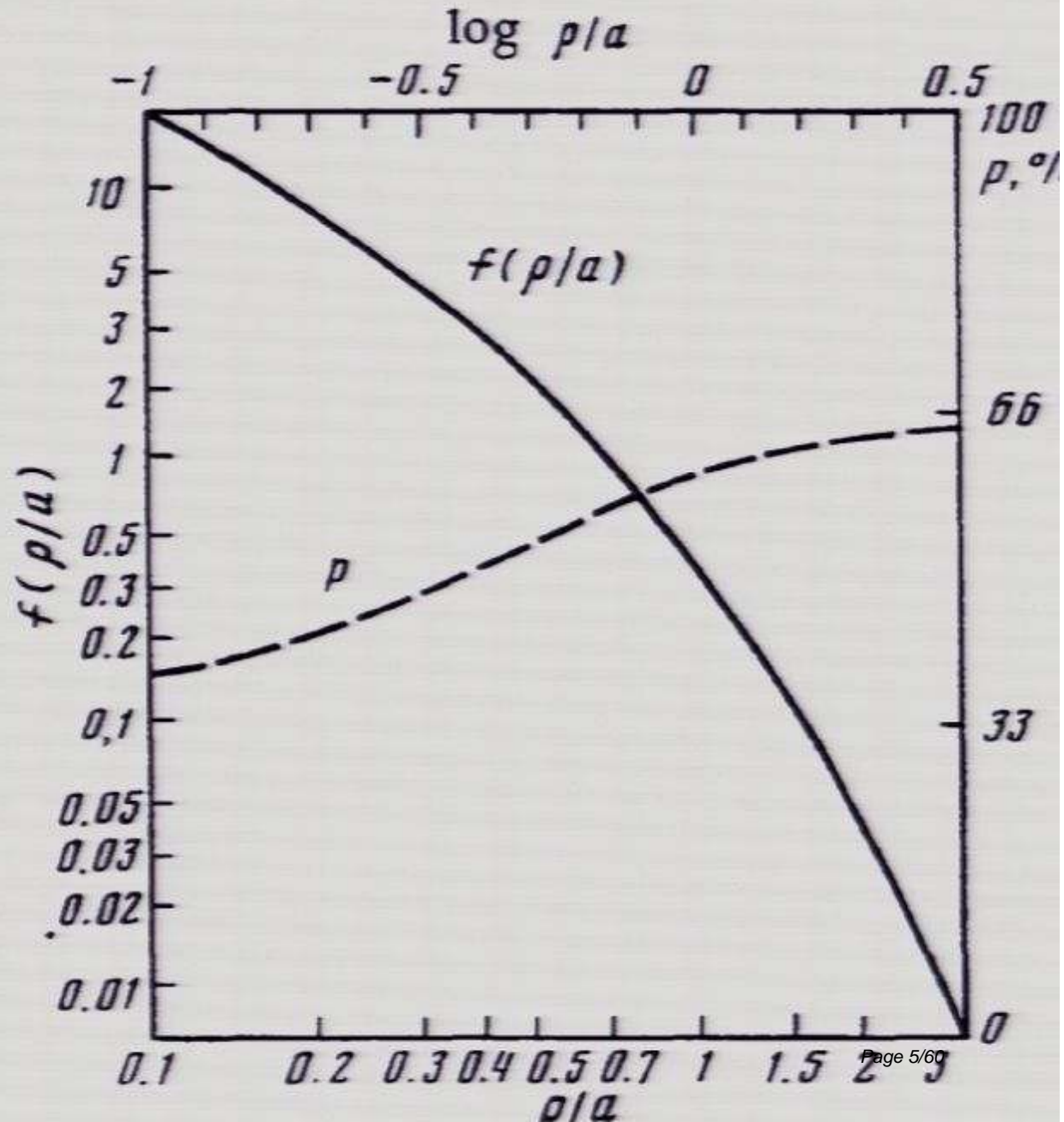
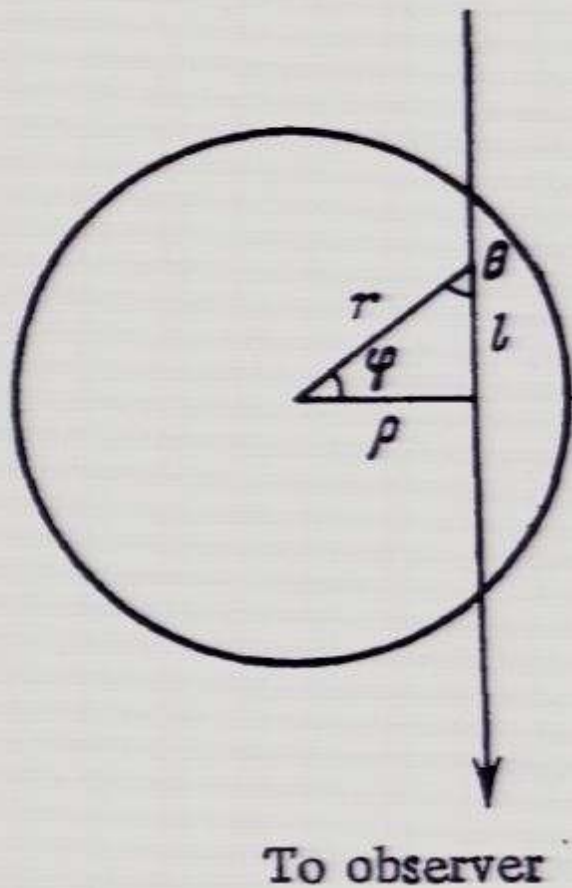
# SRG – observing strategy

<p>All-sky survey (41253 deg<sup>2</sup>): continuous scan with revolution around the axis tilted to Sun direction at ~30° per 96 minute (=orbit)</p>	<p>4 years</p>
<p>Deep Survey and pointed observations of individual objects</p>	<p>3–6 years</p>

# Bright source in the cluster

# Polarization of the scattered radiation

Scattering on free electrons



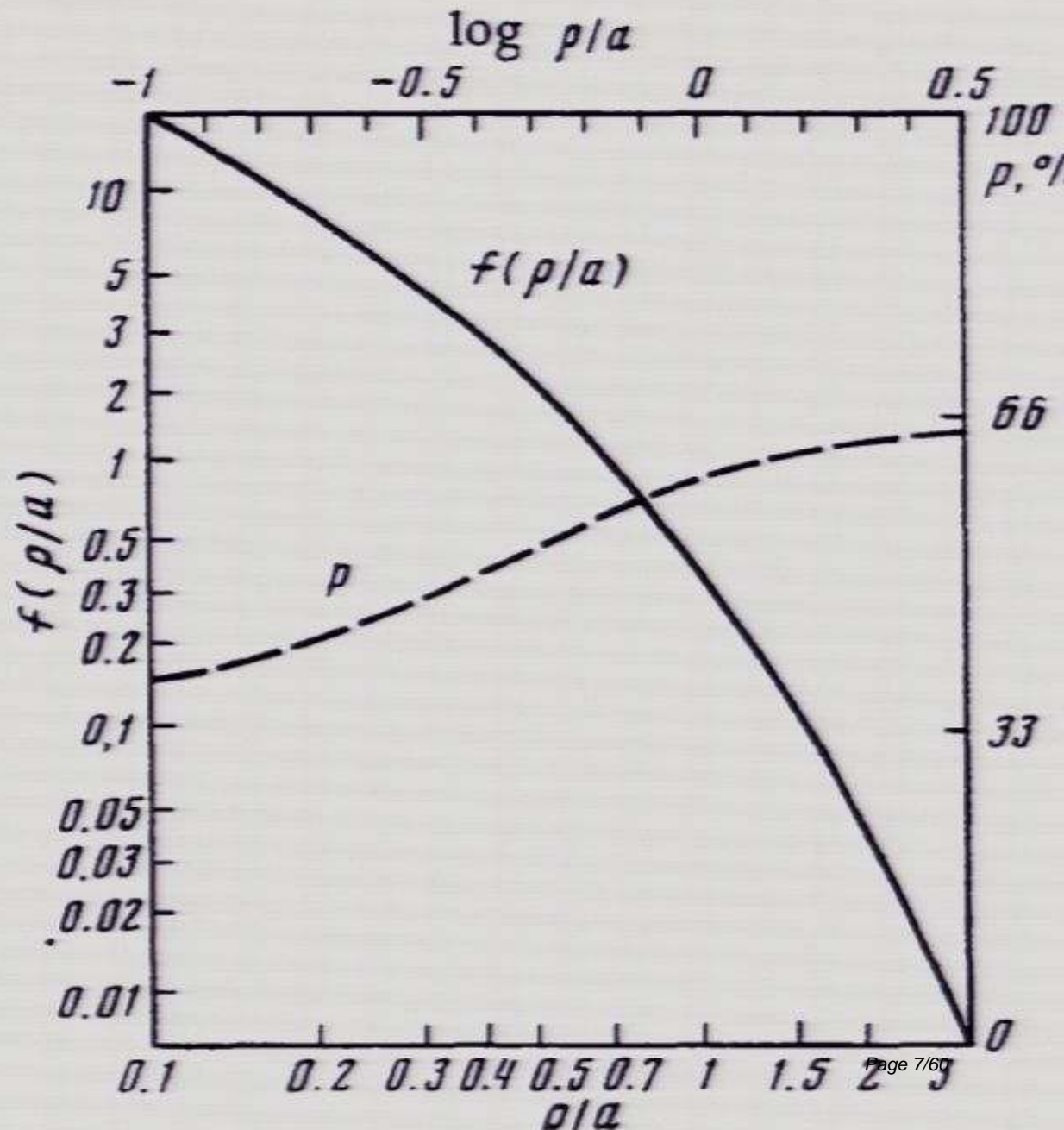
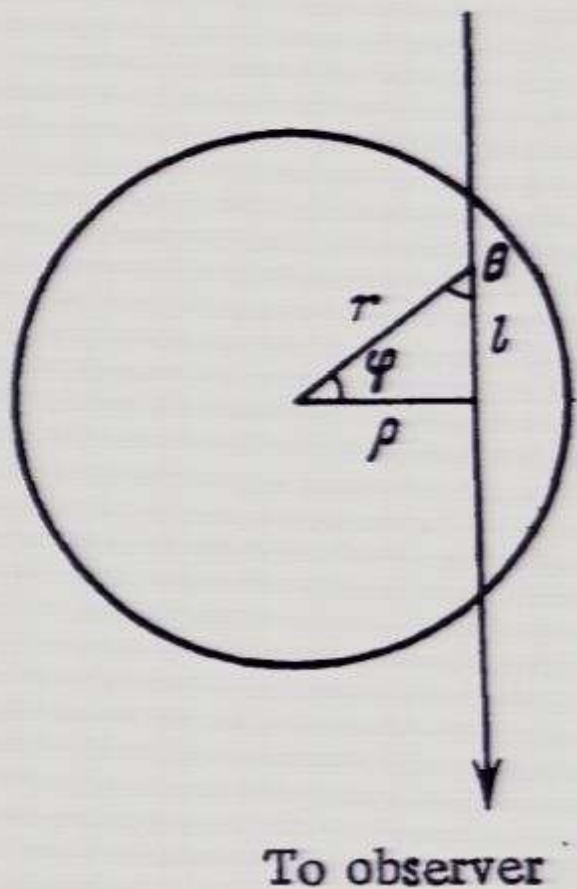
# SRG – observing strategy

<p>All-sky survey (41253 deg<sup>2</sup>): continuous scan with revolution around the axis tilted to Sun direction at ~30° per 96 minute (=orbit)</p>	<p>4 years</p>
<p>Deep Survey and pointed observations of individual objects</p>	<p>3–6 years</p>

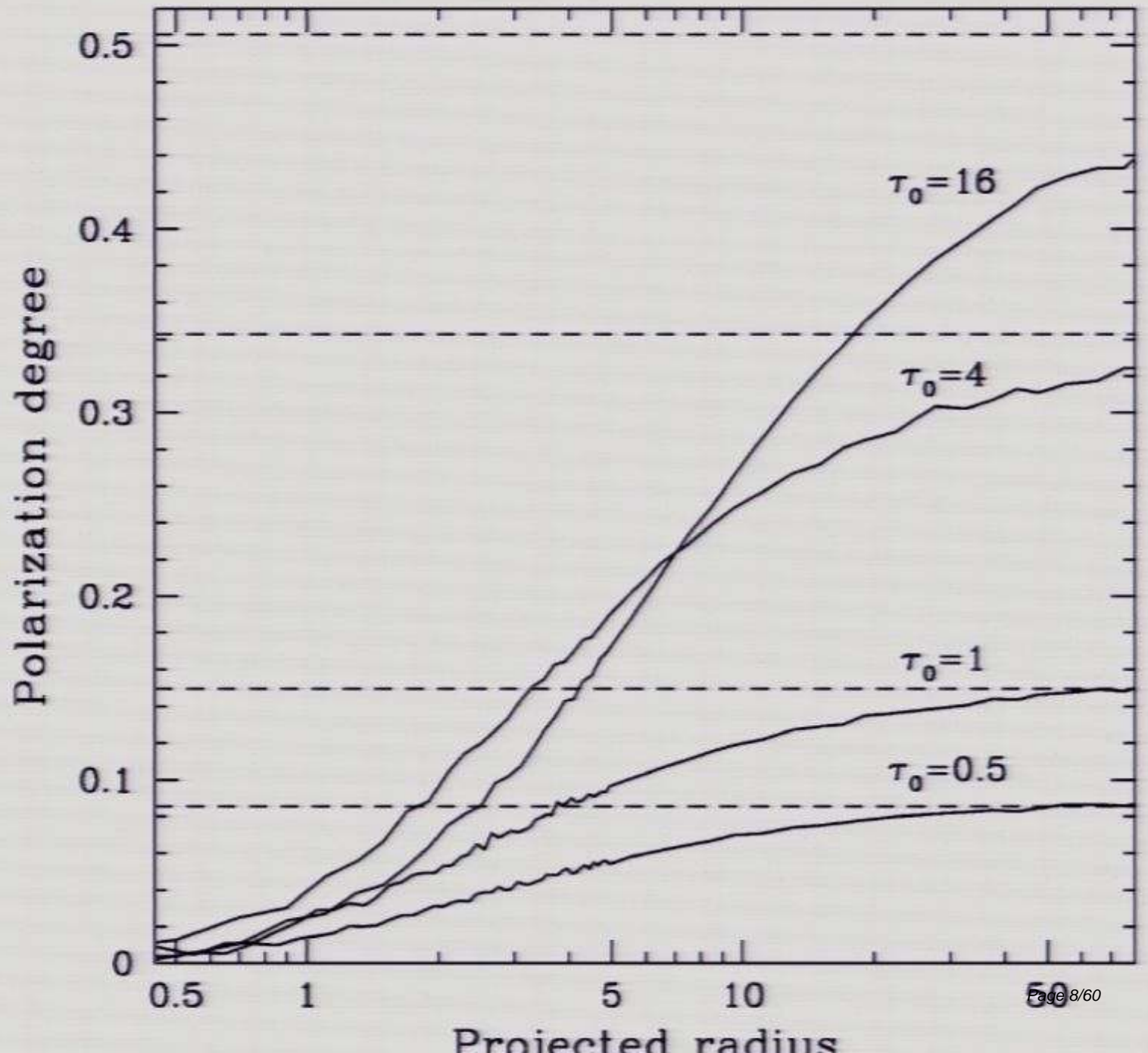
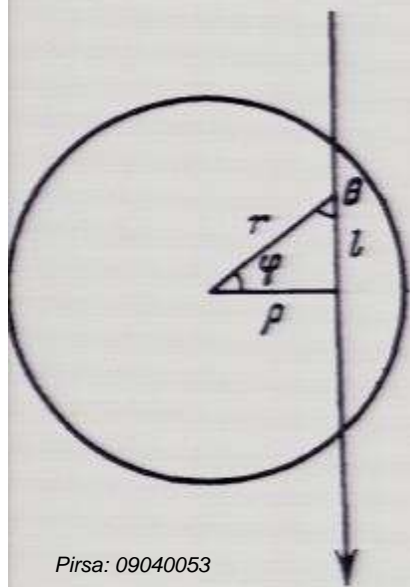
# Bright source in the cluster

# Polarization of the scattered radiation

Scattering on free electrons



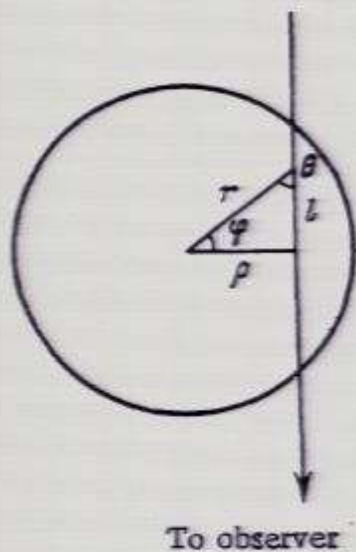
# Scattering in X-Ray resonant lines in the hot gas inside clusters



## Scattering in X-Ray resonant lines in the hote gas inside clusters

*X-Rays are emitted in the central part and scattered in the outer parts of the clusters*

**Table 2.** X-ray lines with large optical depth ( $\tau_0 > 0.5$ ) to resonant scattering: the Perseus cluster.

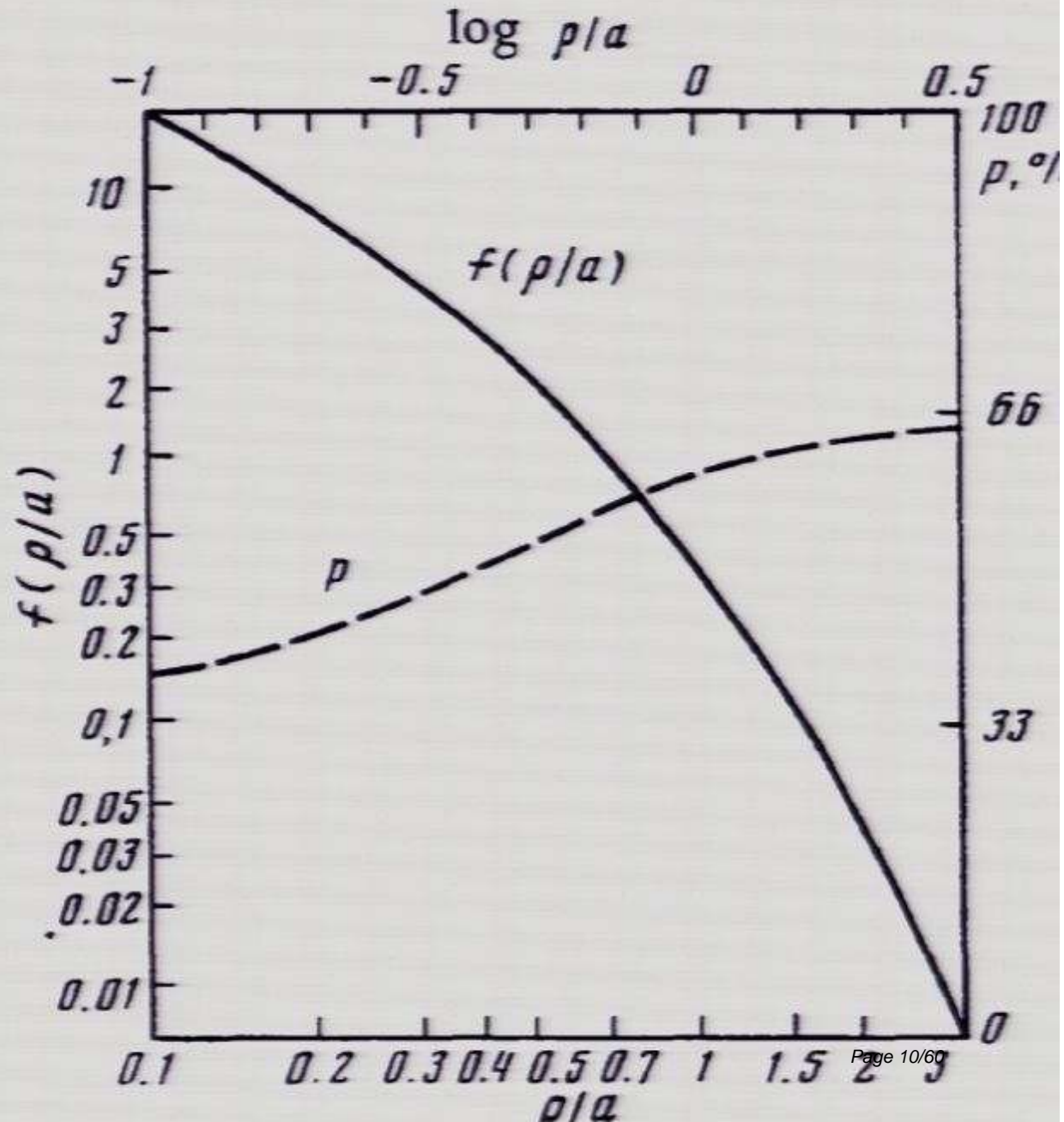
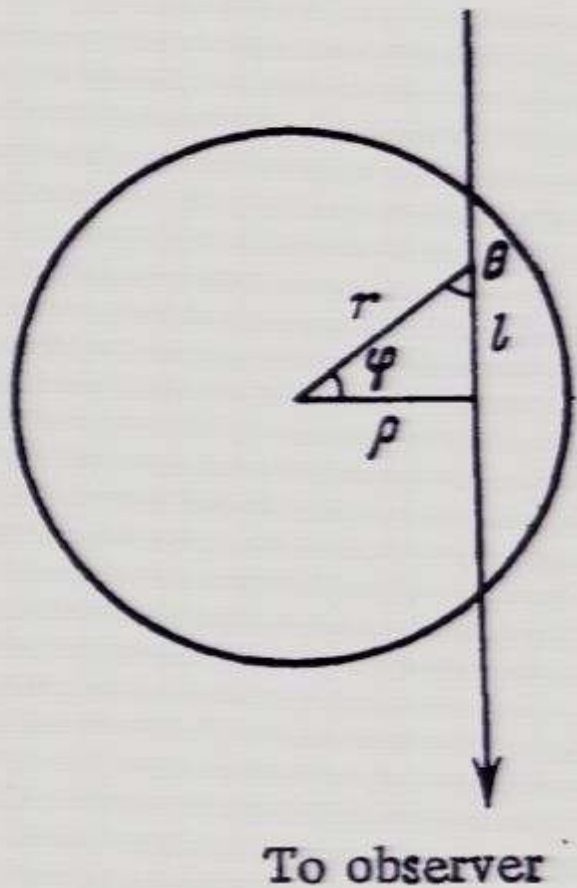


Ion	Energy (keV)	Optical depth	Weight of dipole scattering
Fe XXIV	1.163	0.8	0
Fe XXIV	1.168	1.6	0.5
Fe XXV	6.700	3.3	1
Fe XXV	7.881	0.5	1

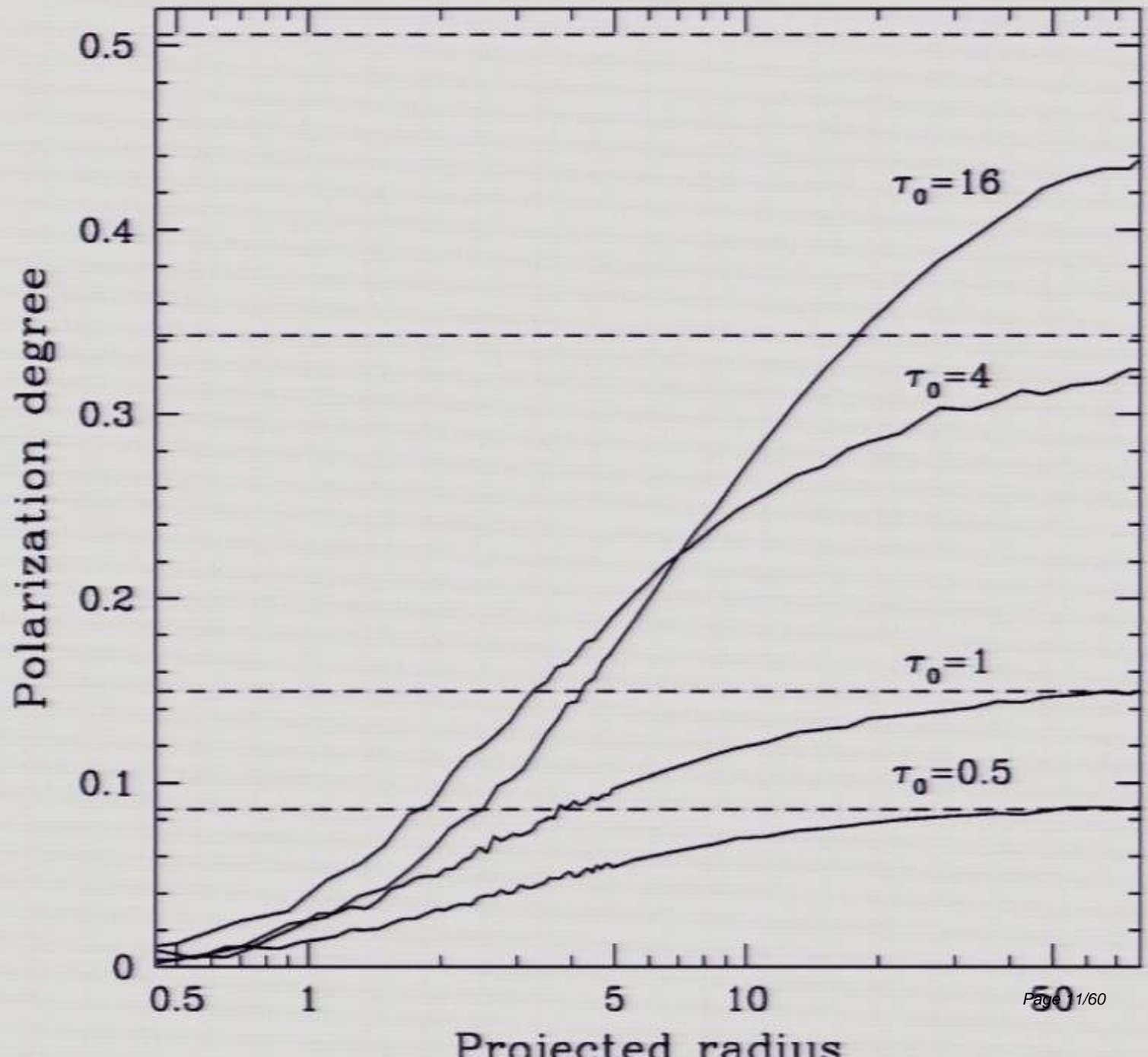
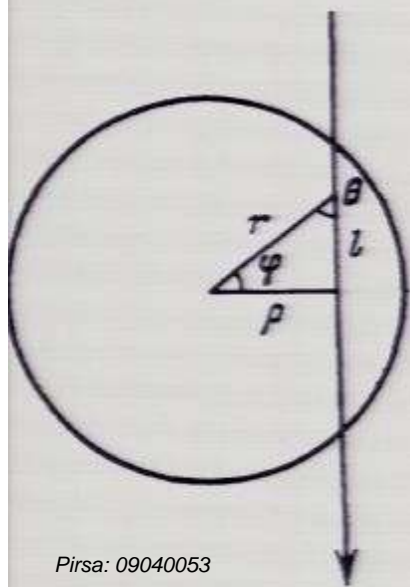
# Bright source in the cluster

# Polarization of the scattered radiation

Scattering on free electrons



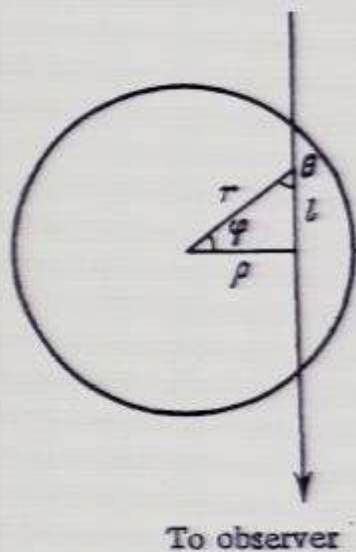
# Scattering in X-Ray resonant lines in the hot gas inside clusters



## Scattering in X-Ray resonant lines in the hote gas inside clusters

*X-Rays are emitted in the central part and scattered in the outer parts of the clusters*

**Table 2.** X-ray lines with large optical depth ( $\tau_0 > 0.5$ ) to resonant scattering: the Perseus cluster.



Ion	Energy (keV)	Optical depth	Weight of dipole scattering
Fe XXIV	1.163	0.8	0
Fe XXIV	1.168	1.6	0.5
Fe XXV	6.700	3.3	1
Fe XXV	7.881	0.5	1

# Perseus Cluster

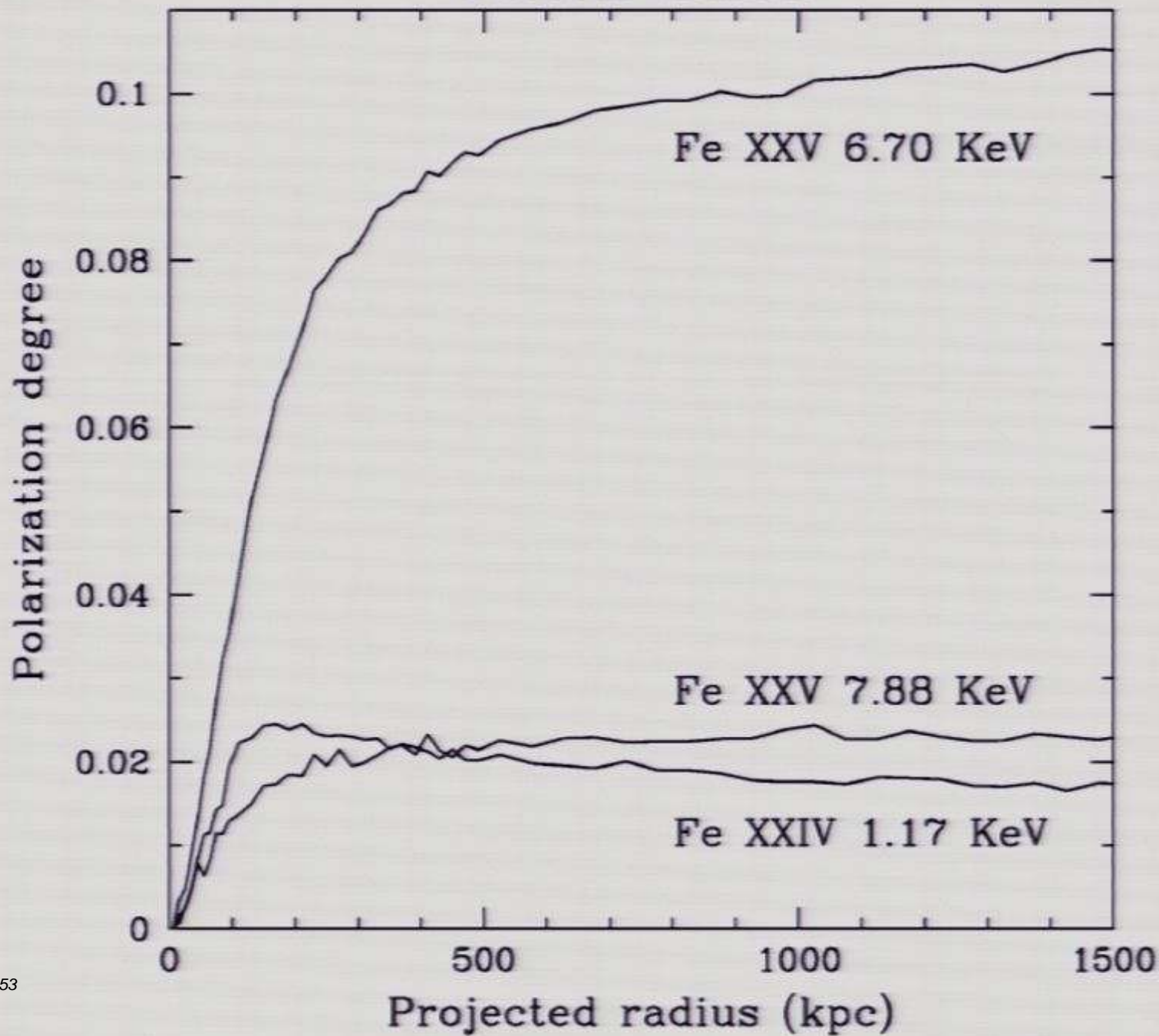


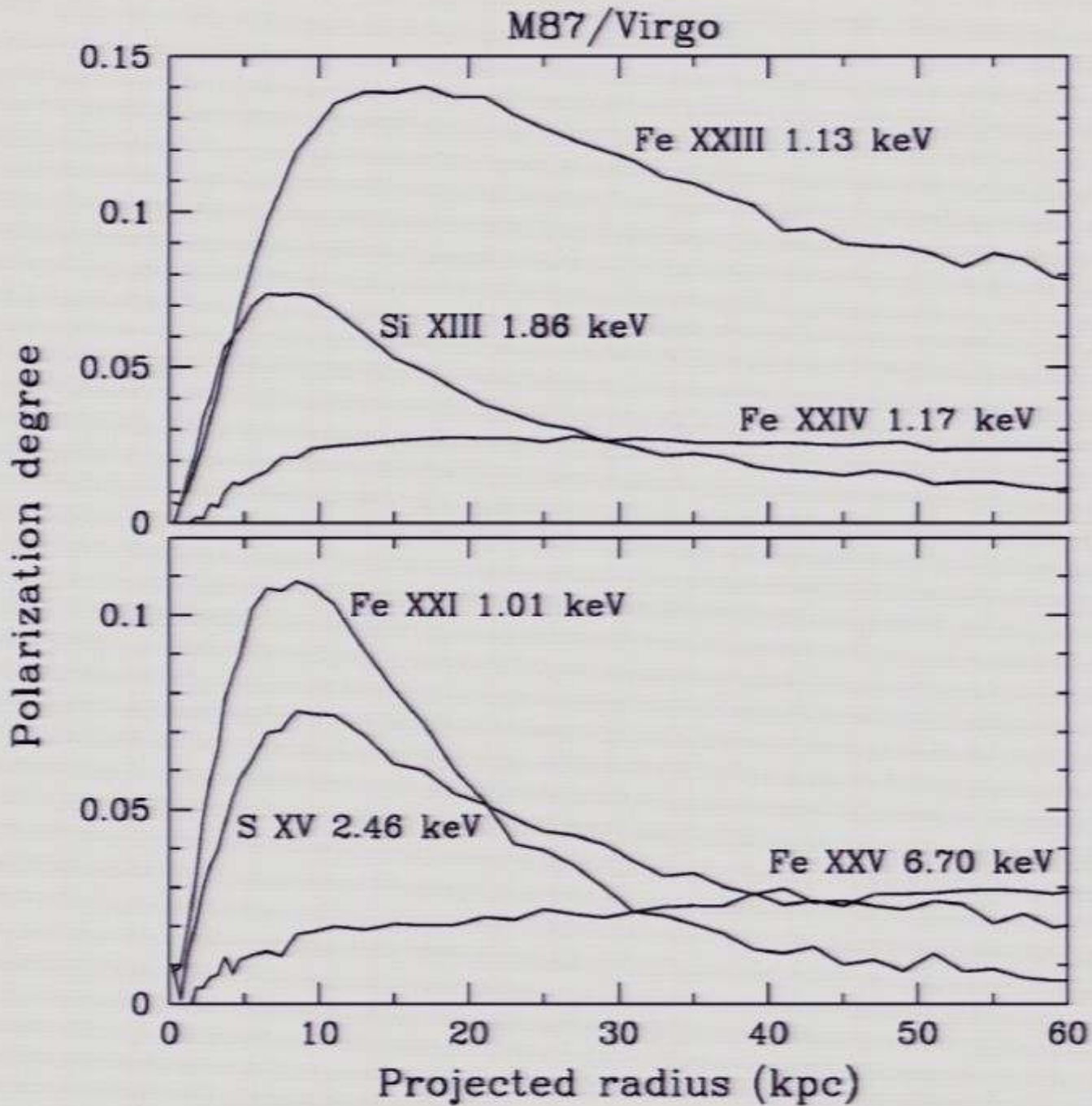
**Table 3.** X-ray lines with large optical depth ( $\tau_0 > 0.5$ ) to resonant scattering: the M87/Virgo cooling flow.

Ion	Energy (keV)	Optical depth	Weight of dipole scattering
O VIII	0.654	0.4	0
O VIII	0.654	0.7	0.5
Ne X	1.021	0.5	0
Ne X	1.022	1.0	0.5
Si XIII	1.865	2.1	1
Si XIV	2.004	0.8	0
Si XIV	2.006	1.7	0.5
S XV	2.461	2.5	1
S XVI	2.620	0.3	0
S XVI	2.623	0.6	0.5
Ar XVII	3.140	0.8	1
Fe XX	0.967	0.7	0.28
Fe XX	0.967	0.5	0.32
Fe XXI	1.009	2.3	1
Fe XXII	1.053	3.3	0.5
Fe XXII	1.064	0.5	0
Fe XXII	1.084	1.5	0.5
Fe XXIII	1.129	6.2	1
Fe XXIII	1.493	1.2	1
Fe XXIV	1.163	1.6	0
Fe XXIV	1.168	3.2	0.5
Fe XXIV	1.553	0.6	0.5
Fe XXV	6.700	1.8	1

**Table 3.** X-ray lines with large optical depth ( $\tau_0 > 0.5$ ) to resonant scattering: the M87/Virgo cool flow.

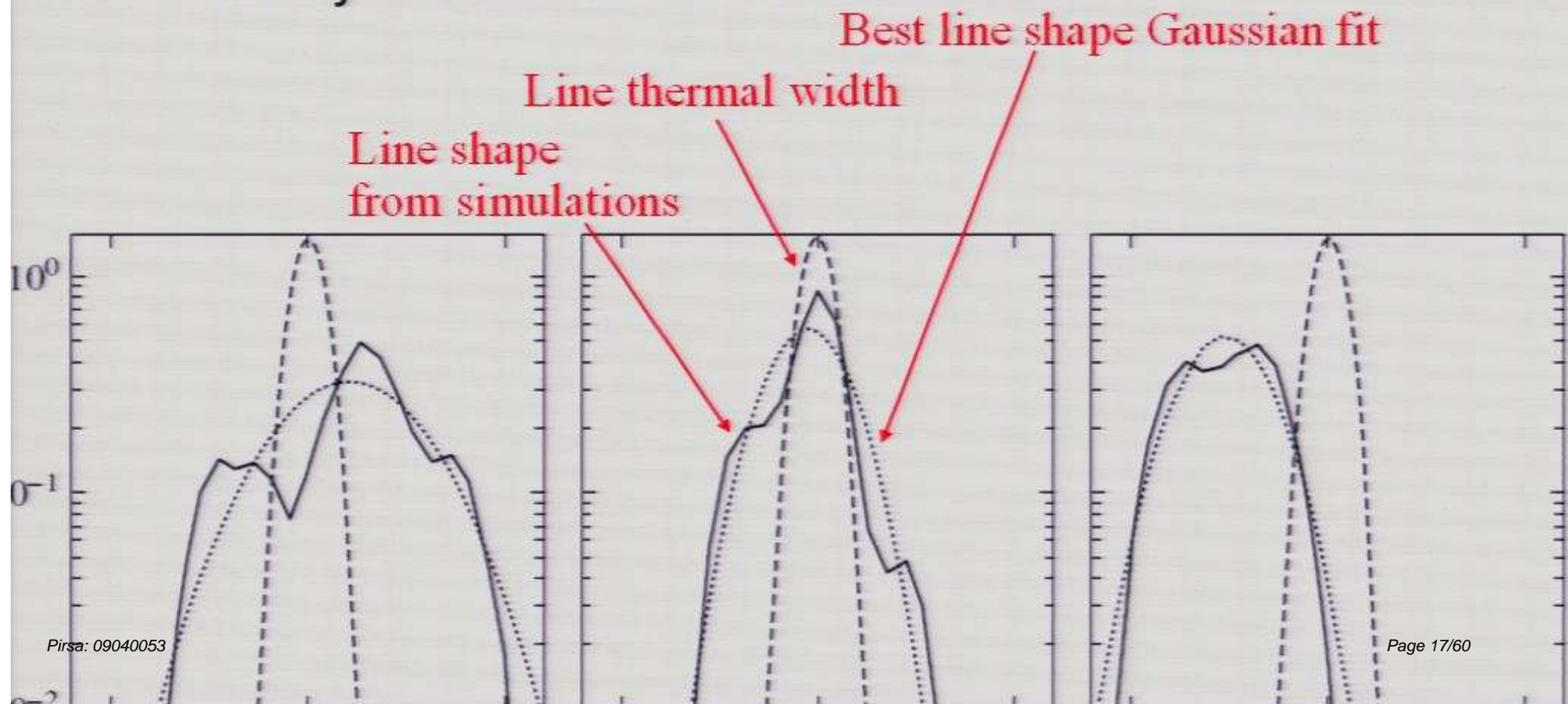
Ion	Energy (keV)	Optical depth	Weight of dipole scattering
O VIII	0.654	0.4	0
O VIII	0.654	0.7	0.5
Ne X	1.021	0.5	0
Ne X	1.022	1.0	0.5
Si XIII	1.865	2.1	1
Si XIV	2.004	0.8	0
Si XIV	2.006	1.7	0.5
S XV	2.461	2.5	1
S XVI	2.620	0.3	0
S XVI	2.623	0.6	0.5

S XVI	2.620	0.3	0
S XVI	2.623	0.6	0.5
Ar XVII	3.140	0.8	1
Fe XX	0.967	0.7	0.28
Fe XX	0.967	0.5	0.32
Fe XXI	1.009	2.3	1
Fe XXII	1.053	3.3	0.5
Fe XXII	1.064	0.5	0
Fe XXII	1.084	1.5	0.5
Fe XXIII	1.129	6.2	1
Fe XXIII	1.493	1.2	1
Fe XXIV	1.163	1.6	0
Fe XXIV	1.168	3.2	0.5
Fe XXIV	1.553	0.6	0.5
Fe XXV	6.700	1.8	1



# $^{57}\text{Fe}$ XXIV line: science

- Narrow Doppler profile
  - study turbulence and bulk motions



Electron is moving with velocity  $v$  in the CMB radiation field

$$T_0 = T_r \frac{\sqrt{1 - \beta^2}}{1 + \beta \mu_0}$$

Doppler

Quadrupole component

$$T_0 = T_r [1 - \beta \mu_0 + \beta^2 (\mu_0^2 - 1/3) + \dots]$$

Tangential component  
of velocity

$$p = 0.1 \tau \beta_t^2$$

Linear polarization

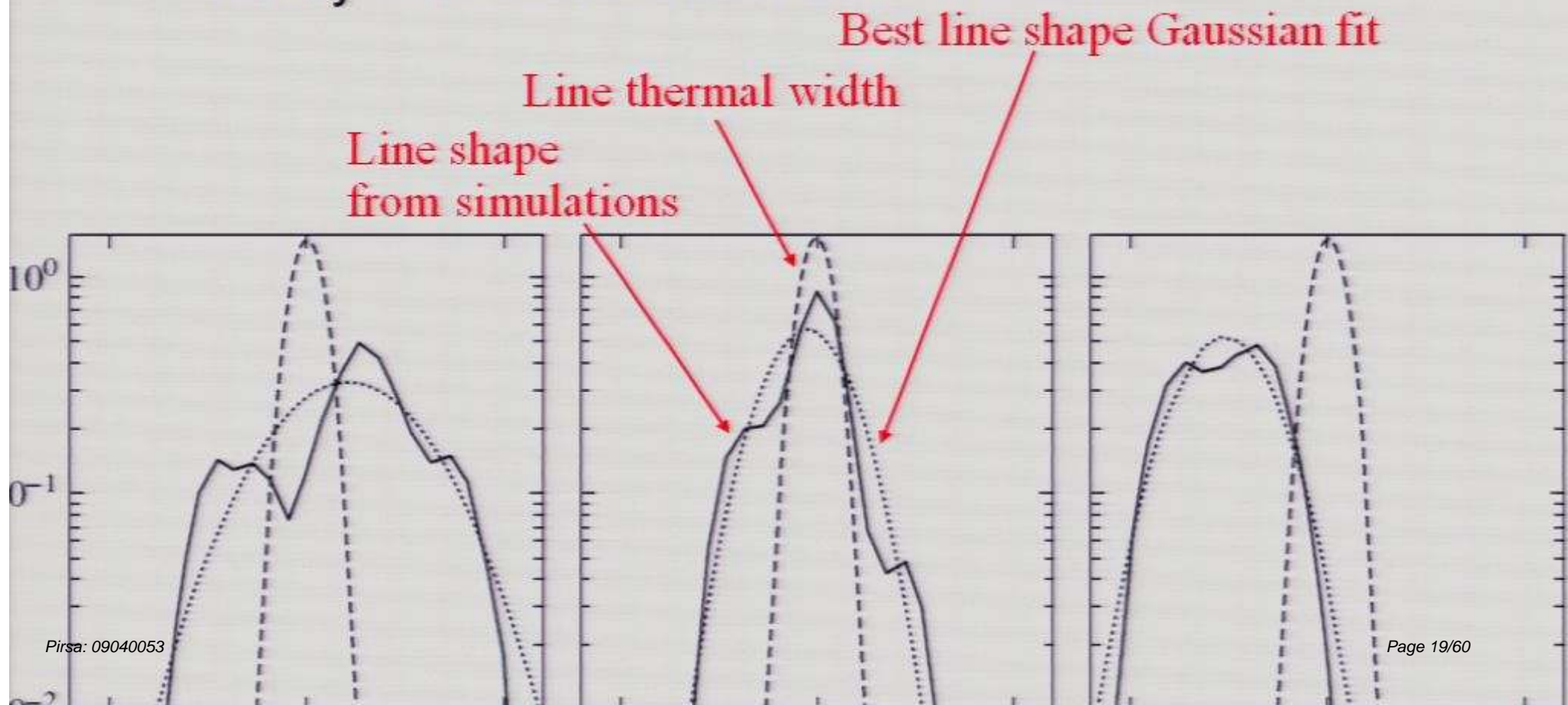
Optical depth

$$p_{\max} = \pm \frac{k}{40} \tau^2 \beta_t$$

Double scatterings also produce  
quadrupole and polarisation

# $^{57}\text{Fe}$ XXIV line: science

- Narrow Doppler profile
  - study turbulence and bulk motions



Electron is moving with velocity  $v$  in the CMB radiation field

$$T_0 = T_r \frac{\sqrt{1 - \beta^2}}{1 + \beta \mu_0}$$

Doppler

Quadrupole component

$$T_0 = T_r [1 - \beta \mu_0 + \beta^2 (\mu_0^2 - 1/3) + \dots]$$

Tangential component  
of velocity

$$p = 0.1 \tau \beta_t^2$$

Linear polarization

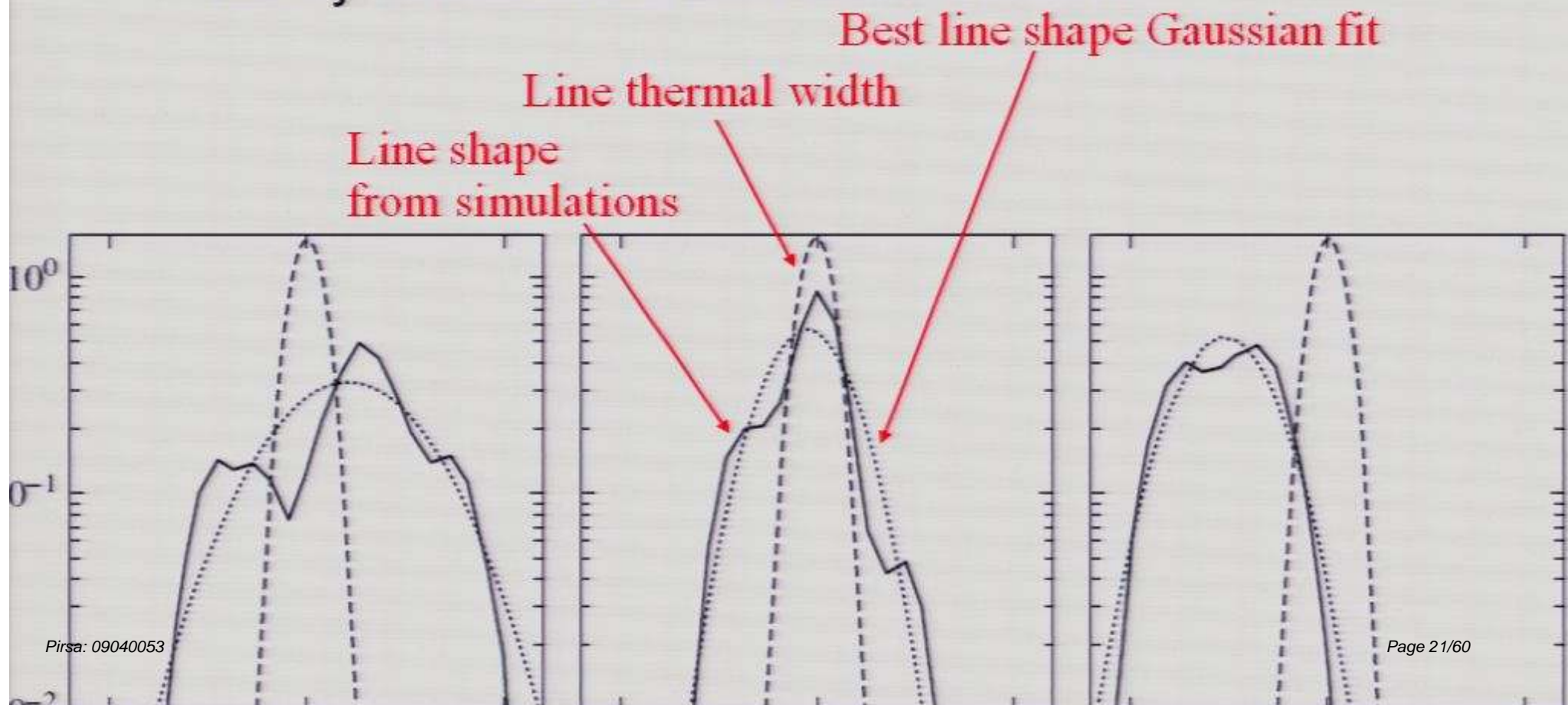
Optical depth

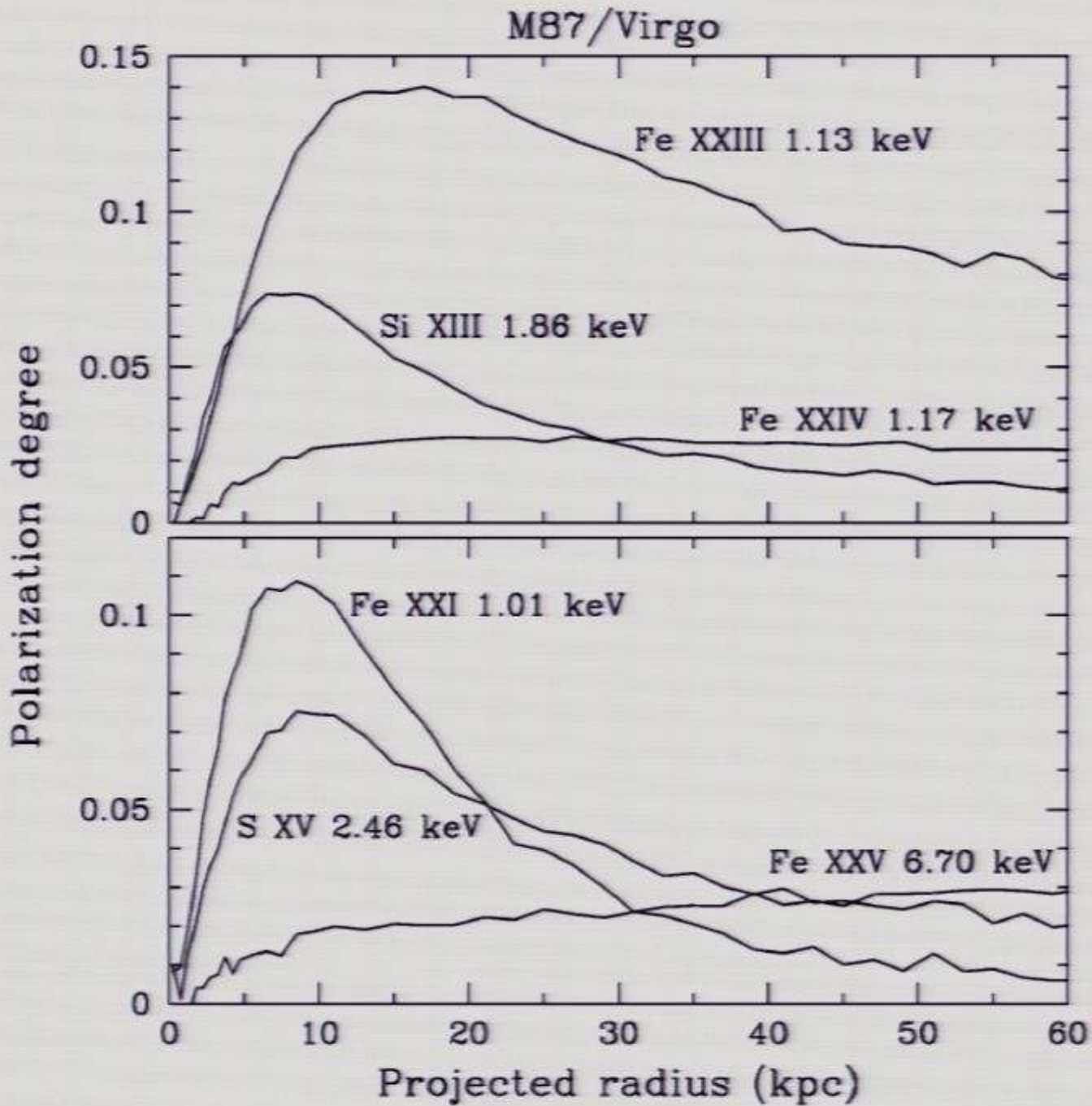
$$p_{\max} = \pm \frac{k}{40} \tau^2 \beta_t$$

Double scatterings also produce  
quadrupole and polarisation

# $^{57}\text{Fe}$ XXIV line: science

- Narrow Doppler profile
  - study turbulence and bulk motions

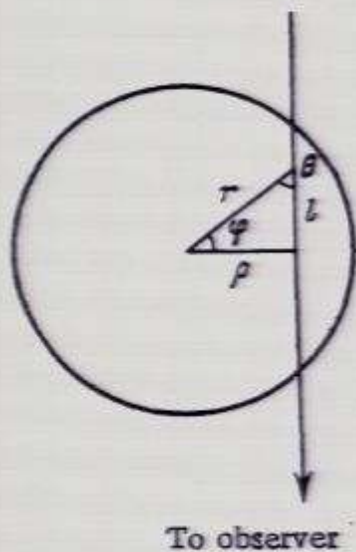




## Scattering in X-Ray resonant lines in the hote gas inside clusters

*X-Rays are emitted in the central part and scattered in the outer parts of the clusters*

**Table 2.** X-ray lines with large optical depth ( $\tau_0 > 0.5$ ) to resonant scattering: the Perseus cluster.



Ion	Energy (keV)	Optical depth	Weight of dipole scattering
Fe XXIV	1.163	0.8	0
Fe XXIV	1.168	1.6	0.5
Fe XXV	6.700	3.3	1
Fe XXV	7.881	0.5	1

**Table 3.** X-ray lines with large optical depth ( $\tau_0 > 0.5$ ) to resonant scattering: the M87/Virgo cool flow.

Ion	Energy (keV)	Optical depth	Weight of dipole scattering
O VIII	0.654	0.4	0
O VIII	0.654	0.7	0.5
Ne X	1.021	0.5	0
Ne X	1.022	1.0	0.5
Si XIII	1.865	2.1	1
Si XIV	2.004	0.8	0
Si XIV	2.006	1.7	0.5
S XV	2.461	2.5	1
S XVI	2.620	0.3	0
S XVI	2.623	0.6	0.5

S XVI	2.620	0.3	0
S XVI	2.623	0.6	0.5
Ar XVII	3.140	0.8	1
Fe XX	0.967	0.7	0.28
Fe XX	0.967	0.5	0.32
Fe XXI	1.009	2.3	1
Fe XXII	1.053	3.3	0.5
Fe XXII	1.064	0.5	0
Fe XXII	1.084	1.5	0.5
Fe XXIII	1.129	6.2	1
Fe XXIII	1.493	1.2	1
Fe XXIV	1.163	1.6	0
Fe XXIV	1.168	3.2	0.5
Fe XXIV	1.553	0.6	0.5
Fe XXV	6.700	1.8	1

Electron is moving with velocity  $v$  in the CMB radiation field

$$T_0 = T_r \frac{\sqrt{1 - \beta^2}}{1 + \beta \mu_0}$$

Doppler

Quadrupole component

$$T_0 = T_r [1 - \beta \mu_0 + \beta^2 (\mu_0^2 - 1/3) + \dots]$$

Tangential component  
of velocity

$$p = 0.1 \tau \beta_t^2$$

Linear polarization

Optical depth

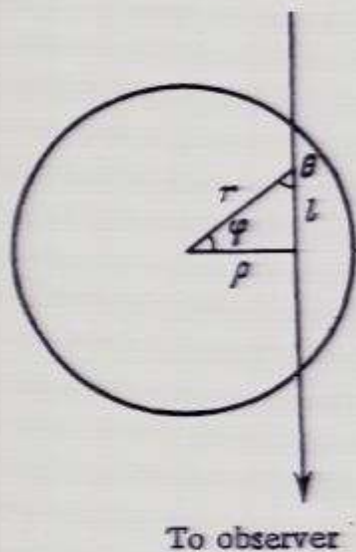
$$p_{\max} = \pm \frac{k}{40} \tau^2 \beta_t$$

Double scatterings also produce  
quadrupole and polarisation

## Scattering in X-Ray resonant lines in the hote gas inside clusters

*X-Rays are emitted in the central part and scattered in the outer parts of the clusters*

**Table 2.** X-ray lines with large optical depth ( $\tau_0 > 0.5$ ) to resonant scattering: the Perseus cluster.



Ion	Energy (keV)	Optical depth	Weight of dipole scattering
Fe XXIV	1.163	0.8	0
Fe XXIV	1.168	1.6	0.5
Fe XXV	6.700	3.3	1
Fe XXV	7.881	0.5	1

Yesterday Komatsu and Mason talks:

Second !!! Bullet cluster,  $y \sim 0.001$ ,  $kTe/mc^2 \sim 1/50$  (10 keV in the whole cluster),  
 $\tau \sim 1/20$ ,  $v/c \sim 0.015$

We could expect  $p \sim 10^{-6}$  for CMB in the direction to this cluster

Electron is moving with velocity  $v$  in the CMB radiation field

$$T_0 = T_r \frac{\sqrt{1 - \beta^2}}{1 + \beta\mu_0}$$

Doppler

Quadrupole component

$$T_0 = T_r [1 - \beta\mu_0 + \beta^2(\mu_0^2 - 1/3) + \dots]$$

Tangential component  
of velocity

$$p = 0.1\tau\beta_t^2$$

Linear polarization

Optical depth

$$p_{\max} = \pm \frac{k}{40} \tau^2 \beta_t$$

Double scatterings also produce  
quadrupole and polarisation

Yesterday Komatsu and Mason talks:

Second !!! Bullet cluster,  $y \sim 0.001$ ,  $kT_e/mc^2 \sim 1/50$  (10 keV in the whole cluster),  
 $\tau \sim 1/20$ ,  $v/c \sim 0.015$

We could expect  $p \sim 10^{-6}$  for CMB in the direction to this cluster

Electron is moving with velocity  $v$  in the CMB radiation field

$$T_0 = T_r \frac{\sqrt{1 - \beta^2}}{1 + \beta\mu_0}$$

Doppler

Quadrupole component

$$T_0 = T_r [1 - \beta\mu_0 + \beta^2(\mu_0^2 - 1/3) + \dots]$$

Tangential component  
of velocity

$$p = 0.1\tau\beta_t^2$$

Linear polarization

Optical depth

$$p_{\max} = \pm \frac{k}{40} \tau^2 \beta_t$$

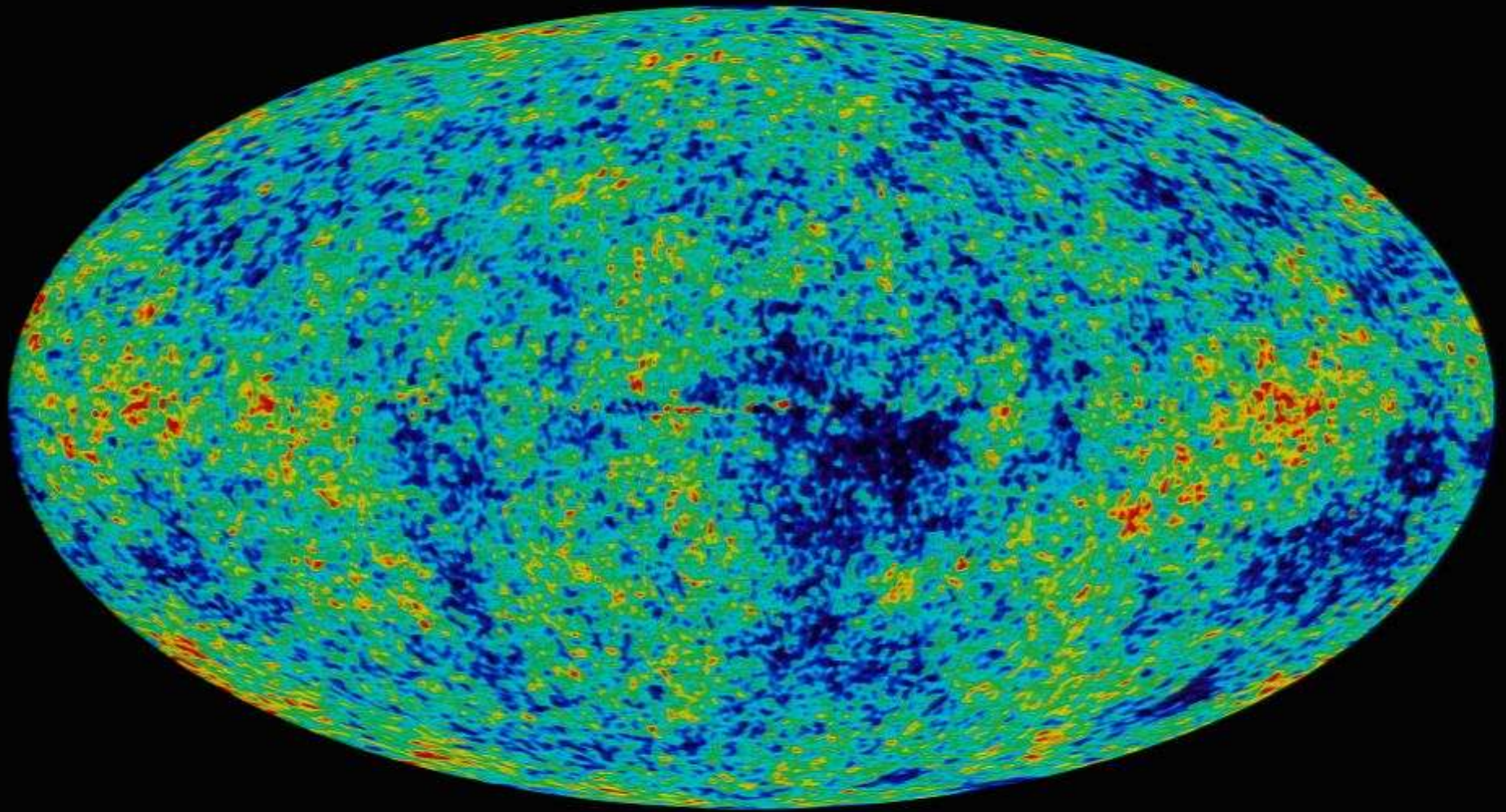
Double scatterings also produce  
quadrupole and polarisation

Yesterday Komatsu and Mason talks:

Second !!! Bullet cluster,  $y \sim 0.001$ ,  $kT_e/mc^2 \sim 1/50$  (10 keV in the whole cluster),  
 $\tau \sim 1/20$ ,  $v/c \sim 0.015$

We could expect  $p \sim 10^{-6}$  for CMB in the direction to this cluster

# Microwave Sky seen by WMAP spacecraft



Dark blue -200 microK

Red +200 microK

CMB (Cosmic Microwave Background) - practically isotropic and has a black spectrum  
Tiny !!! primordial angular fluctuations are of interest

Yesterday Komatsu and Mason talks:

Second !!! Bullet cluster,  $y \sim 0.001$ ,  $kT_e/mc^2 \sim 1/50$  (10 keV in the whole cluster),  
 $\tau \sim 1/20$ ,  $v/c \sim 0.015$

We could expect  $p \sim 10^{-6}$  for CMB in the direction to this cluster

Electron is moving with velocity  $v$  in the CMB radiation field

$$T_0 = T_r \frac{\sqrt{1 - \beta^2}}{1 + \beta\mu_0}$$

Doppler

Quadrupole component

$$T_0 = T_r [1 - \beta\mu_0 + \beta^2(\mu_0^2 - 1/3) + \dots]$$

Tangential component  
of velocity

$$p = 0.1\tau\beta_t^2$$

Linear polarization

Optical depth

$$p_{\max} = \pm \frac{k}{40} \tau^2 \beta_t$$

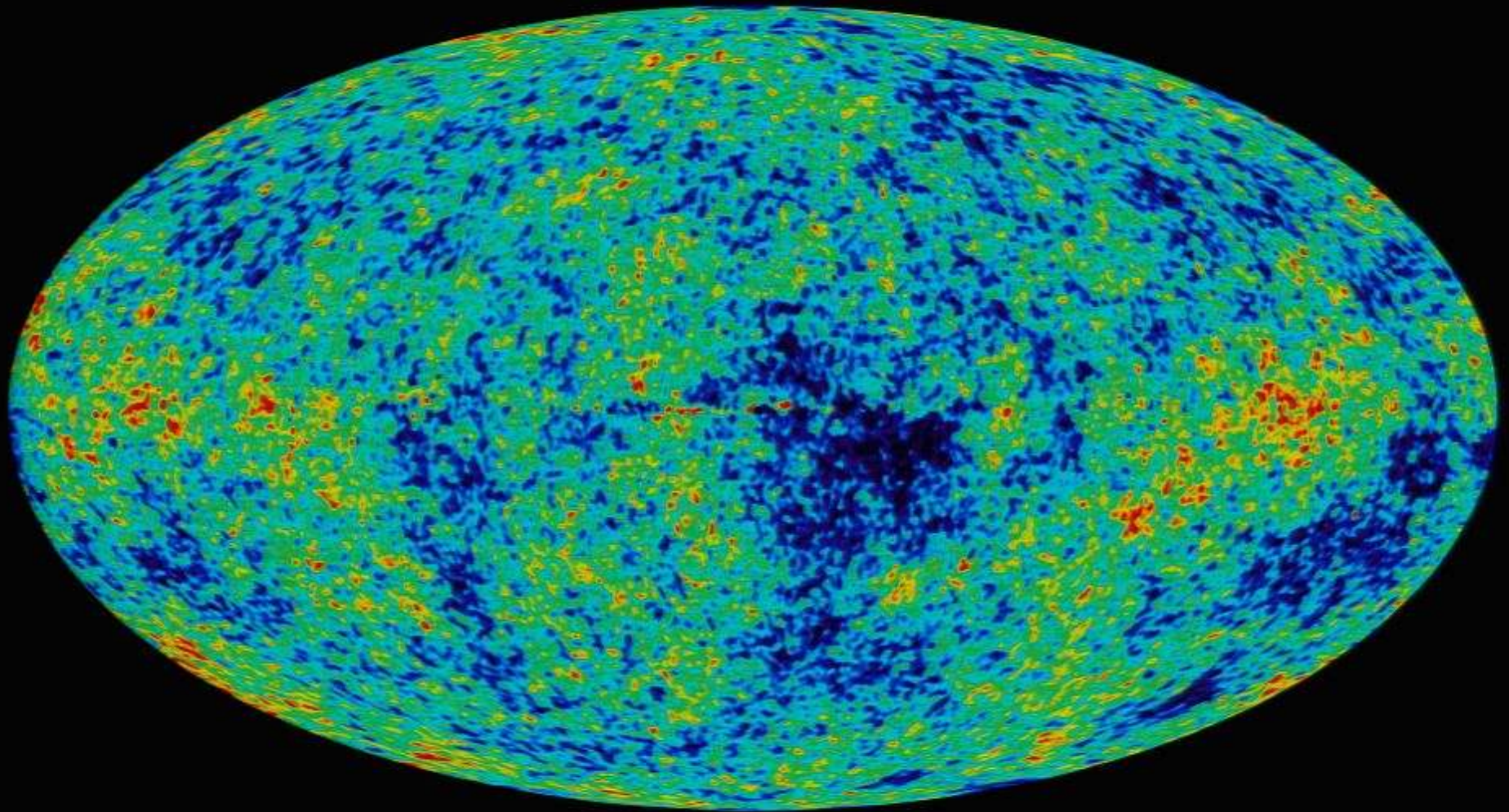
Double scatterings also produce  
quadrupole and polarisation

Yesterday Komatsu and Mason talks:

Second !!! Bullet cluster,  $y \sim 0.001$ ,  $kTe/mc^2 \sim 1/50$  (10 keV in the whole cluster),  
 $\tau \sim 1/20$ ,  $v/c \sim 0.015$

We could expect  $p \sim 10^{-6}$  for CMB in the direction to this cluster

# Microwave Sky seen by WMAP spacecraft



Dark blue -200 microK

Red +200 microK

CMB (Cosmic Microwave Background) - practically isotropic and has a black spectrum  
Tiny !!! primordial angular fluctuations are of interest

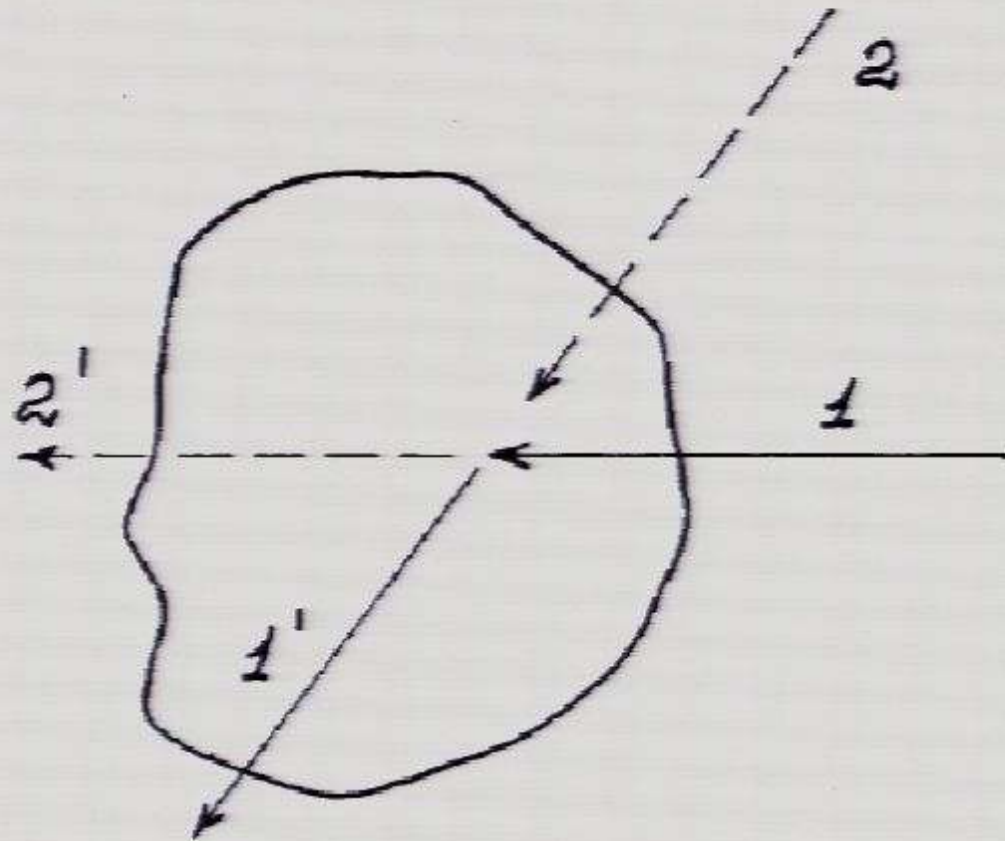


FIG. 2. The scattering of isotropic radiation field by the cloud of electrons.

Cloud is invisible

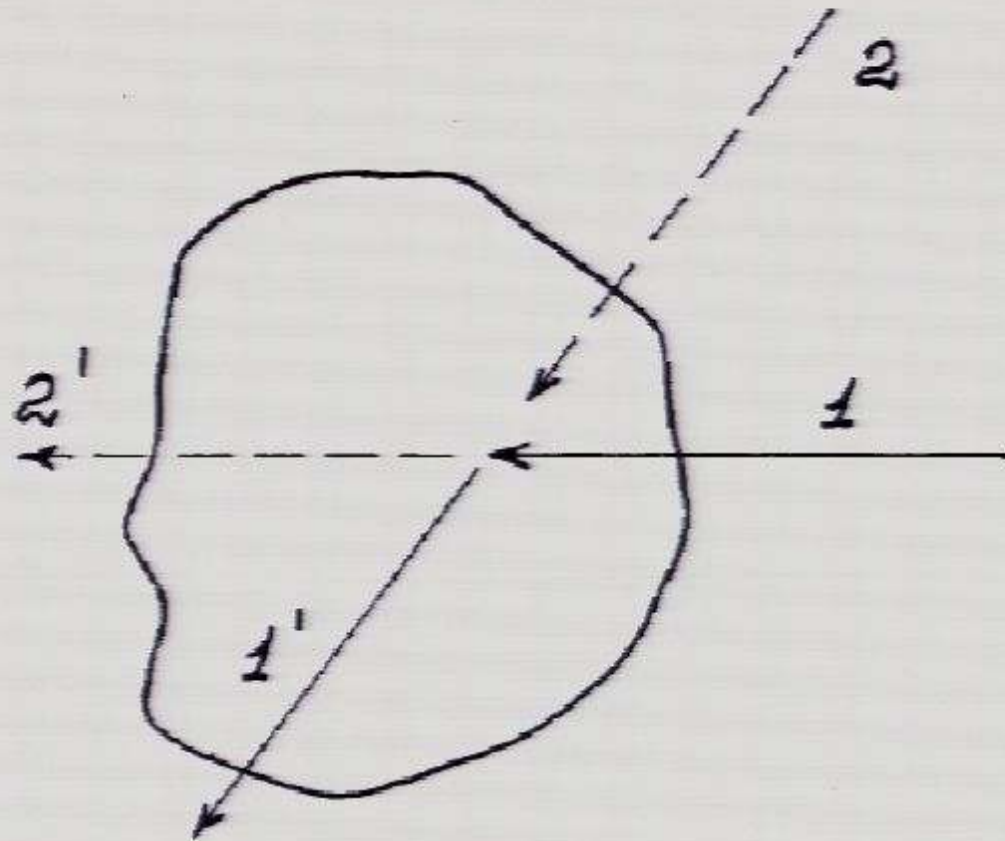
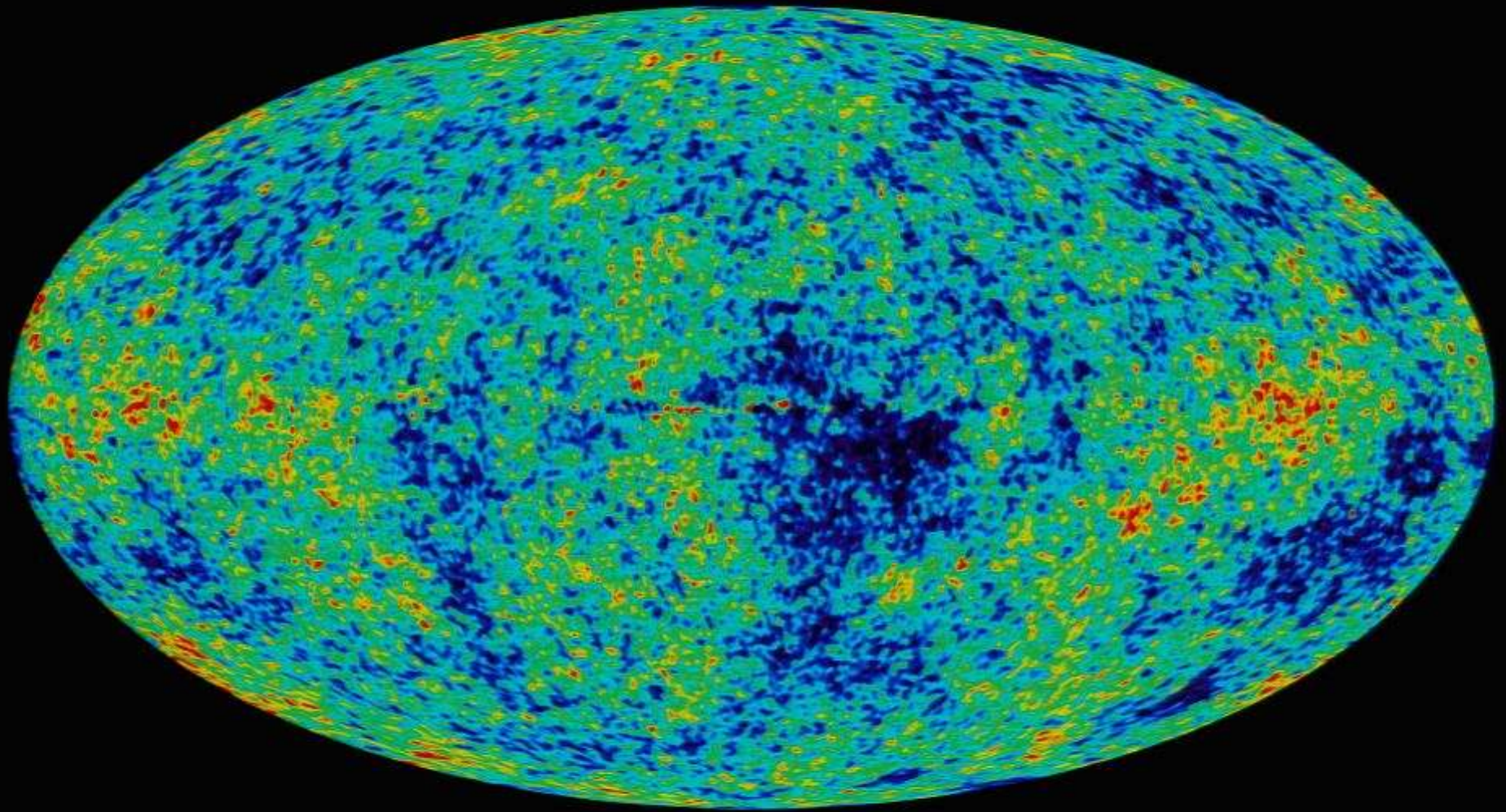


FIG. 2. The scattering of isotropic radiation field by the cloud of electrons.

Cloud is invisible

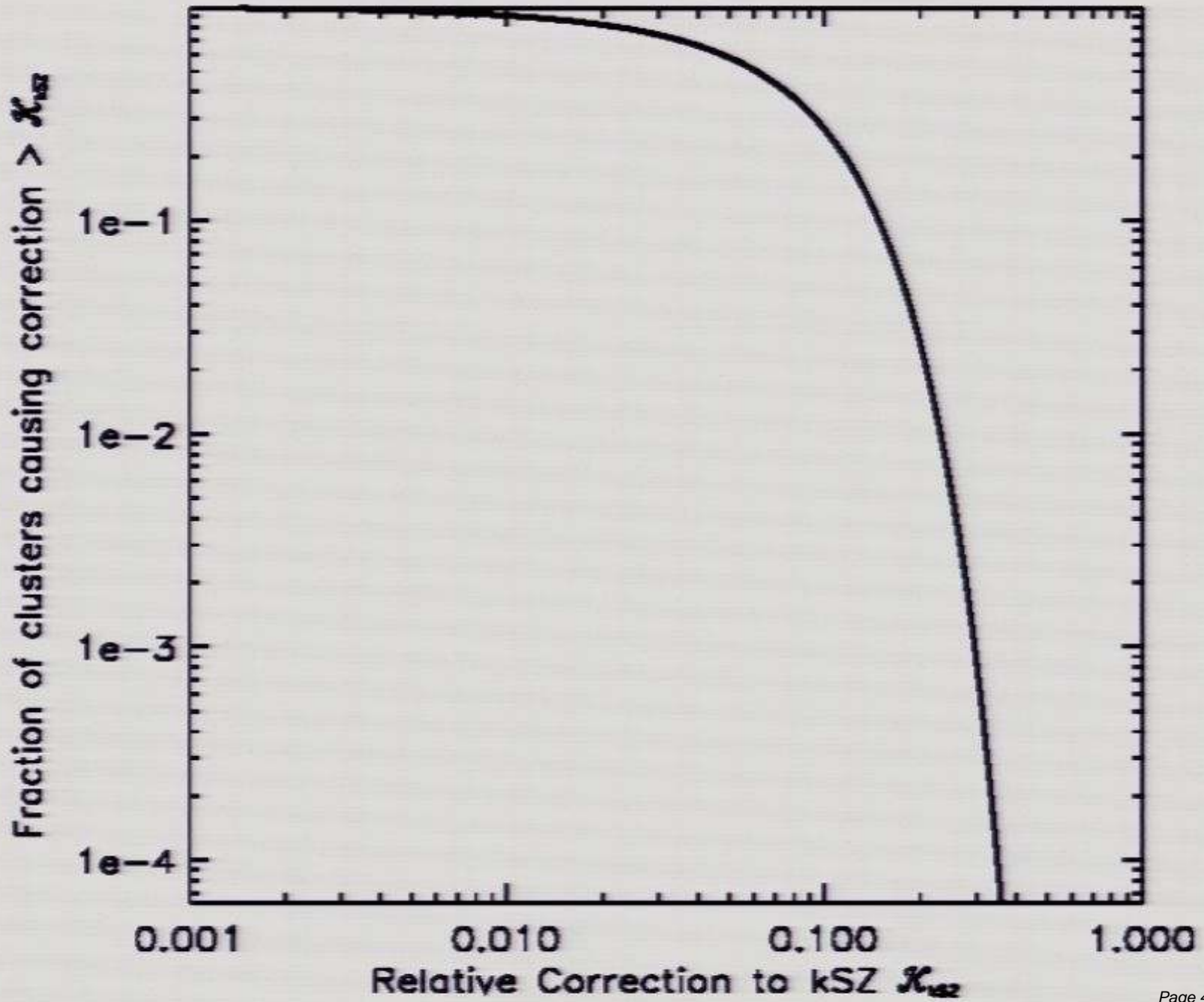
# Microwave Sky seen by WMAP spacecraft

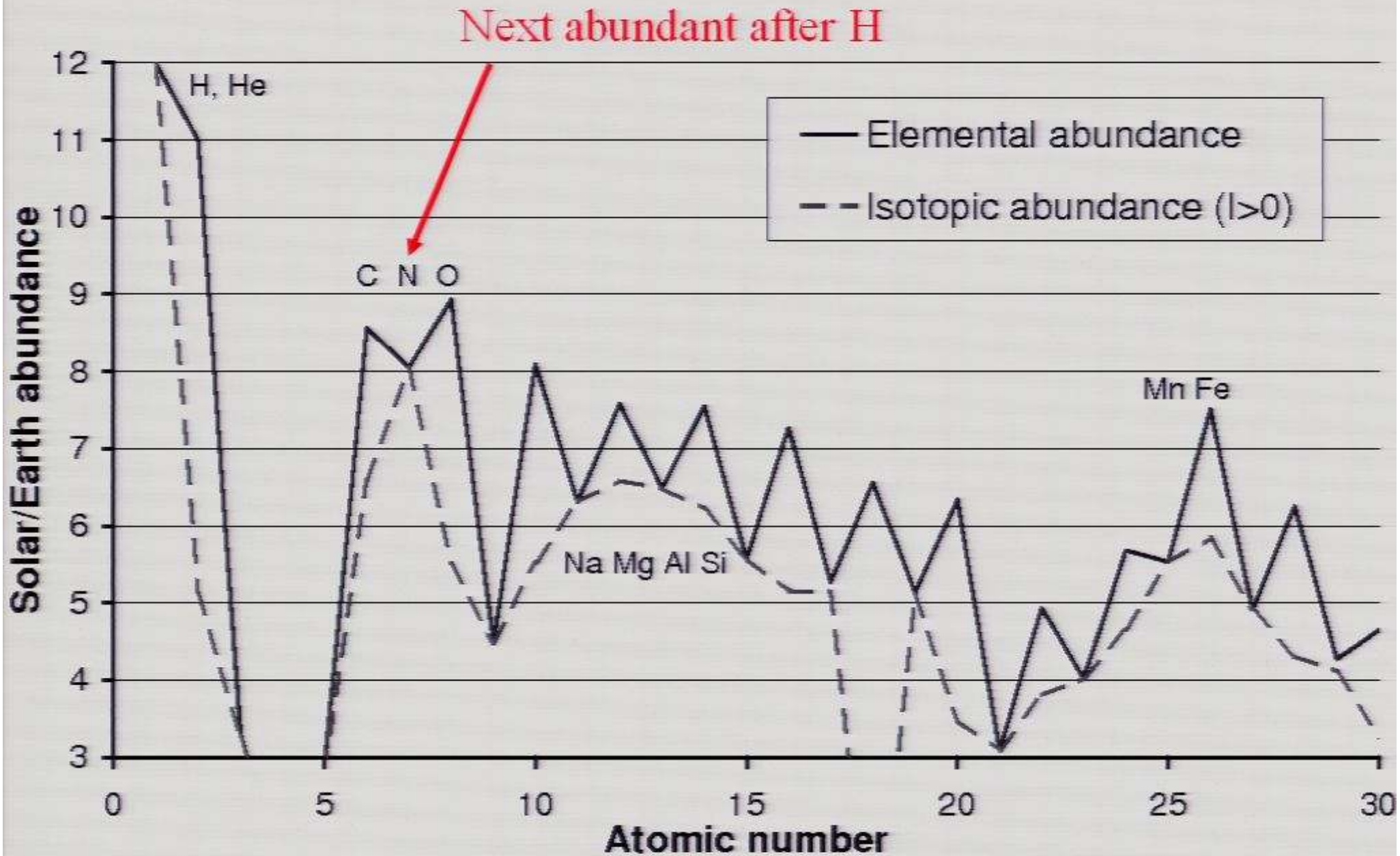


Dark blue -200 microK

Red +200 microK

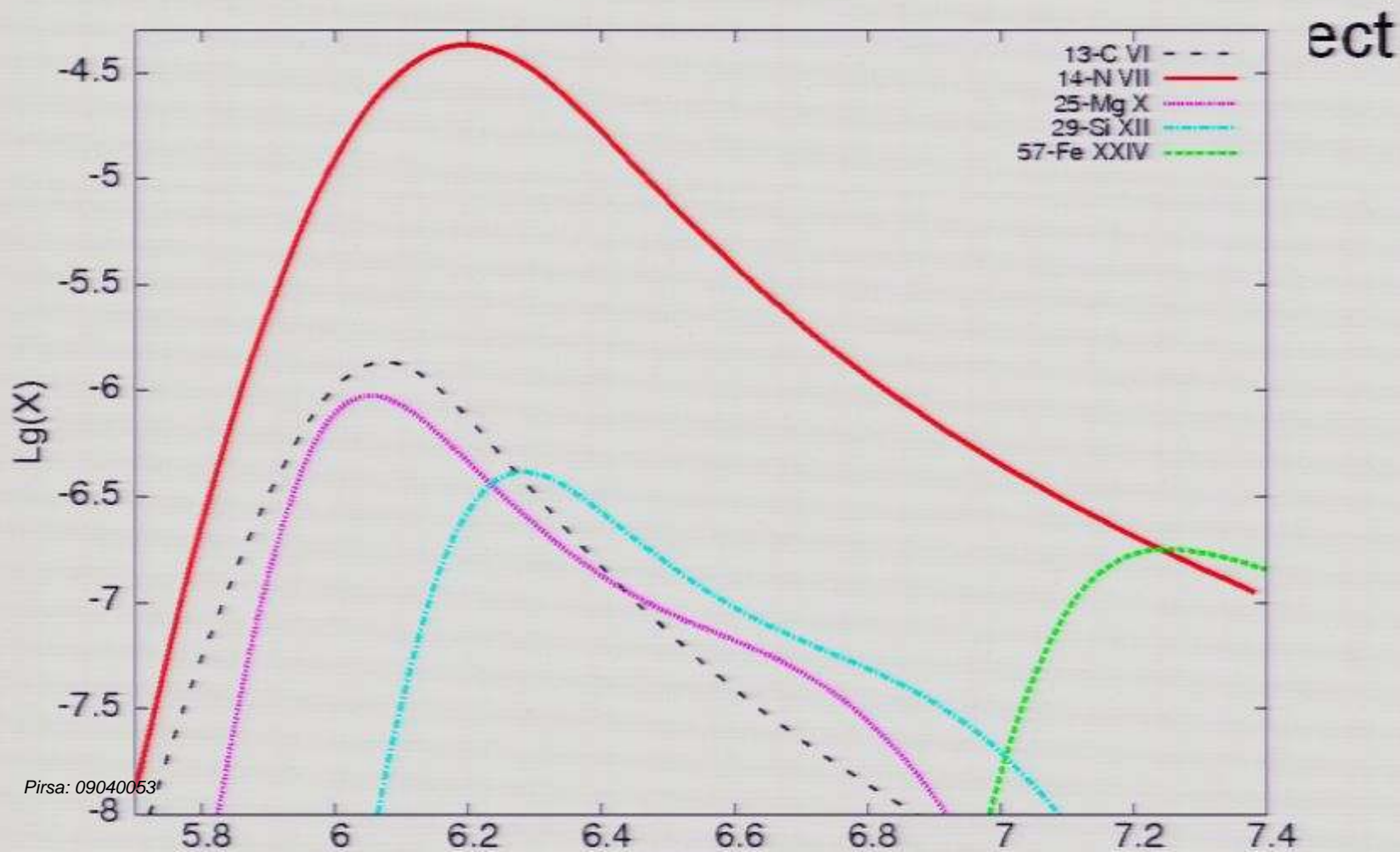
CMB (Cosmic Microwave Background) - practically isotropic and has a black spectrum  
Tiny !!! primordial angular fluctuations are of interest





- HFS transitions are possible only in
  - Isotopes with nuclear spin  $I > 0$ 
    - $^4\text{He}$  has zero nuclear spin
    - All  $\alpha$ -elements ( $^{16}\text{O}$ ,  $^{24}\text{Mg}$ , etc) have zero nuclear spin
    - Lines are especially sensitive to isotopes other than  $\alpha$ -elements
  - Ions with ground state electronic momentum  $J > 0$ 
    - Having one electron around nucleus (three, five etc.)

- Observations of a HFS line determine
  - Plasma temperature, due to ionic abundance
  - Isotopic composition



# Line parameters

- Frequency determined by nuclear charge  $Z$ , magnetic moment and spin  $l$ :

$$\Delta E_{HFS} = \frac{8 \mu}{3 I} \cdot \frac{\alpha^2 Z^3 m_e}{n^3 m_p} \cdot (I + 1/2) Ry$$

- Steep dependence on  $Z$  implies shorter wavelength for high- $Z$  ions

# Line parameters

- Spontaneous decay rate  $A$  is

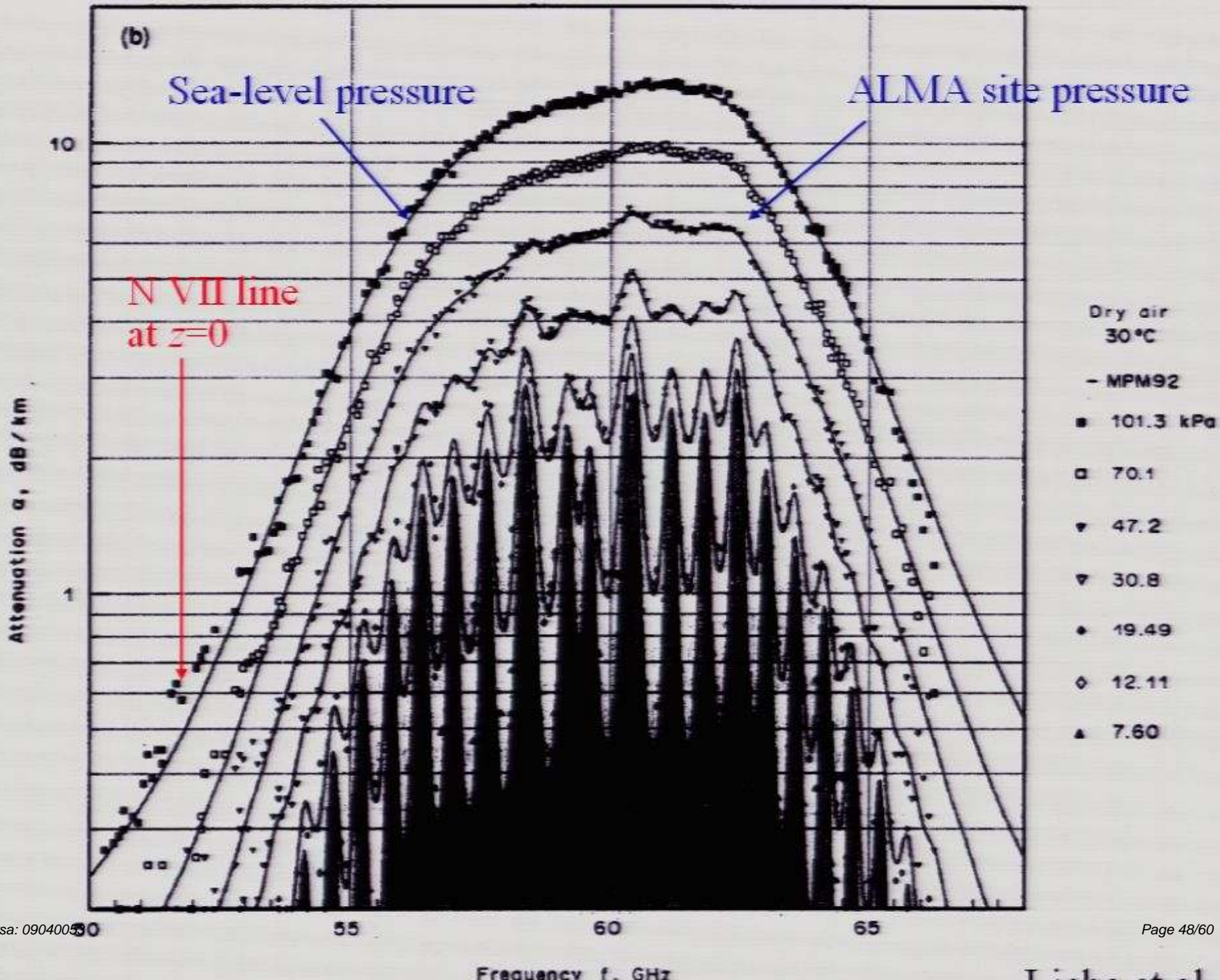
$$\begin{aligned} A(F \rightarrow F - 1) &= \frac{I}{I+1} A(F - 1 \rightarrow F) = \\ &= 1.0789 \cdot 10^{-7} \frac{I}{2I+1} \cdot \left( \frac{\lambda}{1 \text{ mm}} \right)^{-3} \text{ s}^{-1} \end{aligned}$$

- Meaning even sharper dependence on nuclear charge
- This makes high- $Z$  ion HFS lines competitive to the 21 cm line, despite much lower abundances

- Two ways to overcome this
  - Observe from height of ALMA (5100 m), where zenith transmission reaches 30-50%
  - Observe objects with redshift  $z > 0.15$   
(Sunyaev, Churazov 1984)
- Our initial motivation was to choose the latter way
  - To study if the HFS line of  $^{14}\text{N VII}$  may help in detection of the warm-hot intergalactic medium (WHIM)

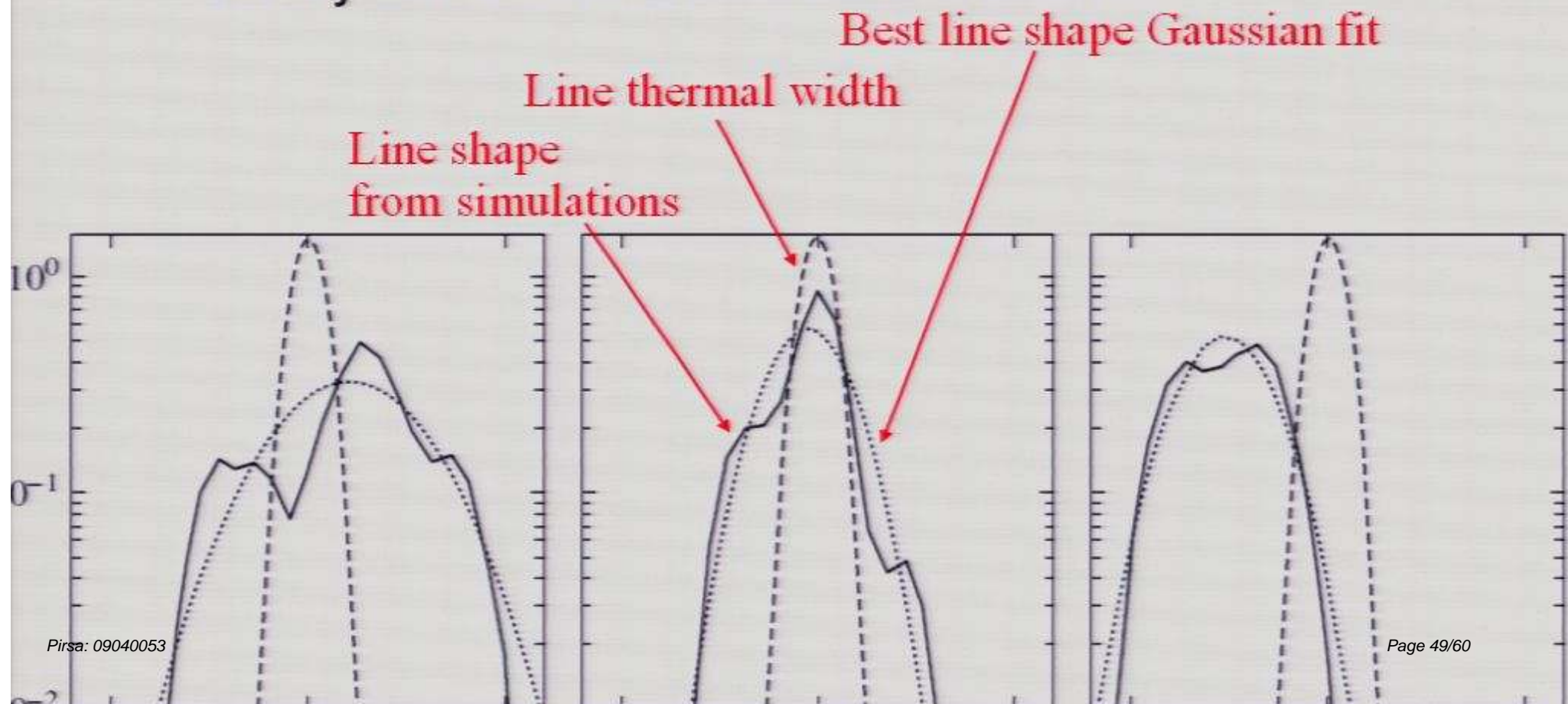
## Line brightness temperature, $\mu\text{K}$

Isotope	$\lambda$ , mm	N157B	CL
$^{13}\text{C}$ VI	3.8740(8)	4	13
$^{14}\text{N}$ VII	5.6519(11)	700	400
$^{17}\text{O}$ VIII	1.0085(2)	0.8	0.08
$^{25}\text{Mg}$ X	6.680(4)	15	14
$^{27}\text{Al}$ XI	1.2060(7)	50	40
$^{29}\text{Si}$ XII	3.725(2)	30	3.0



# $^{57}\text{Fe}$ XXIV line: science

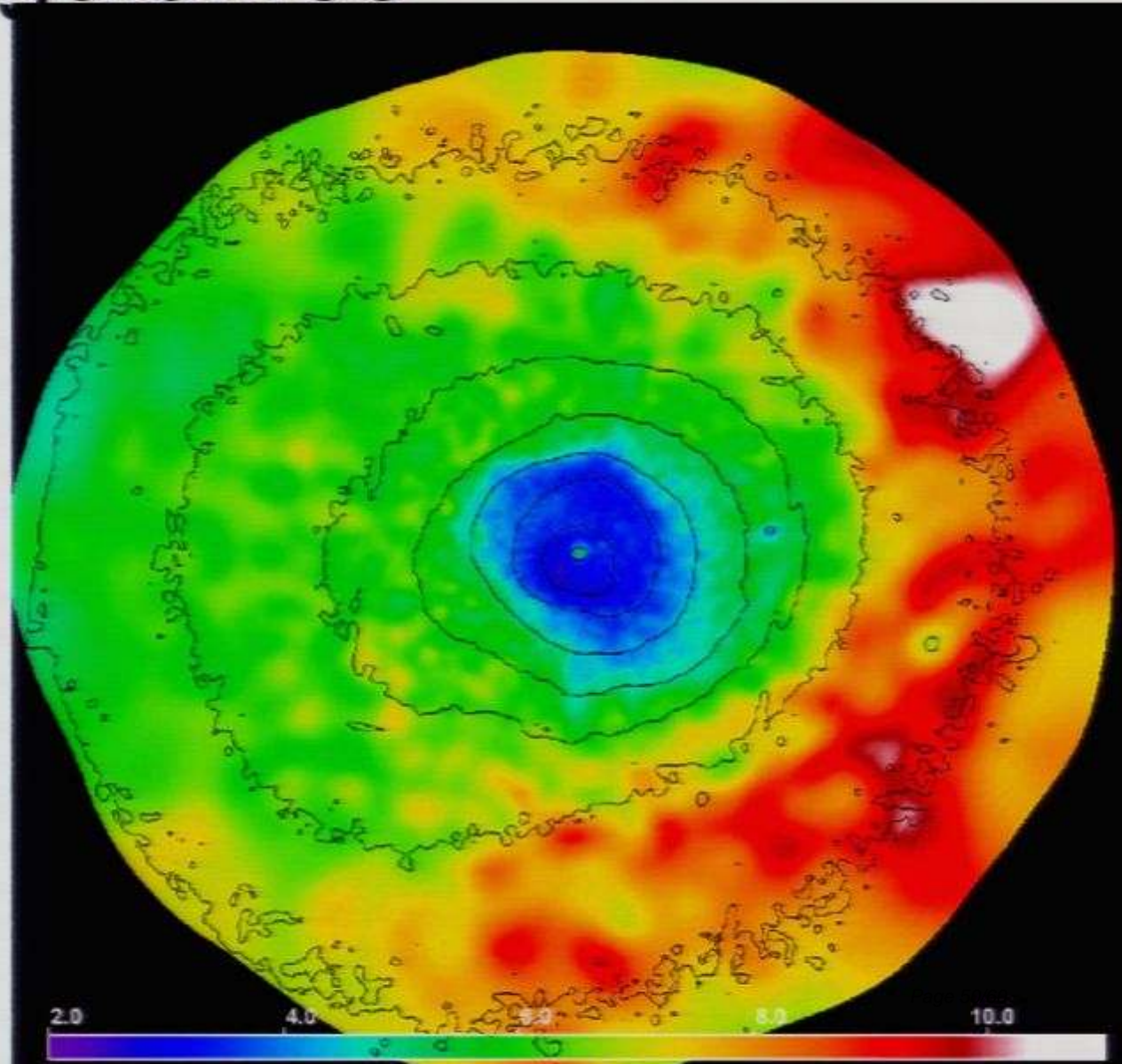
- Narrow Doppler profile
  - study turbulence and bulk motions



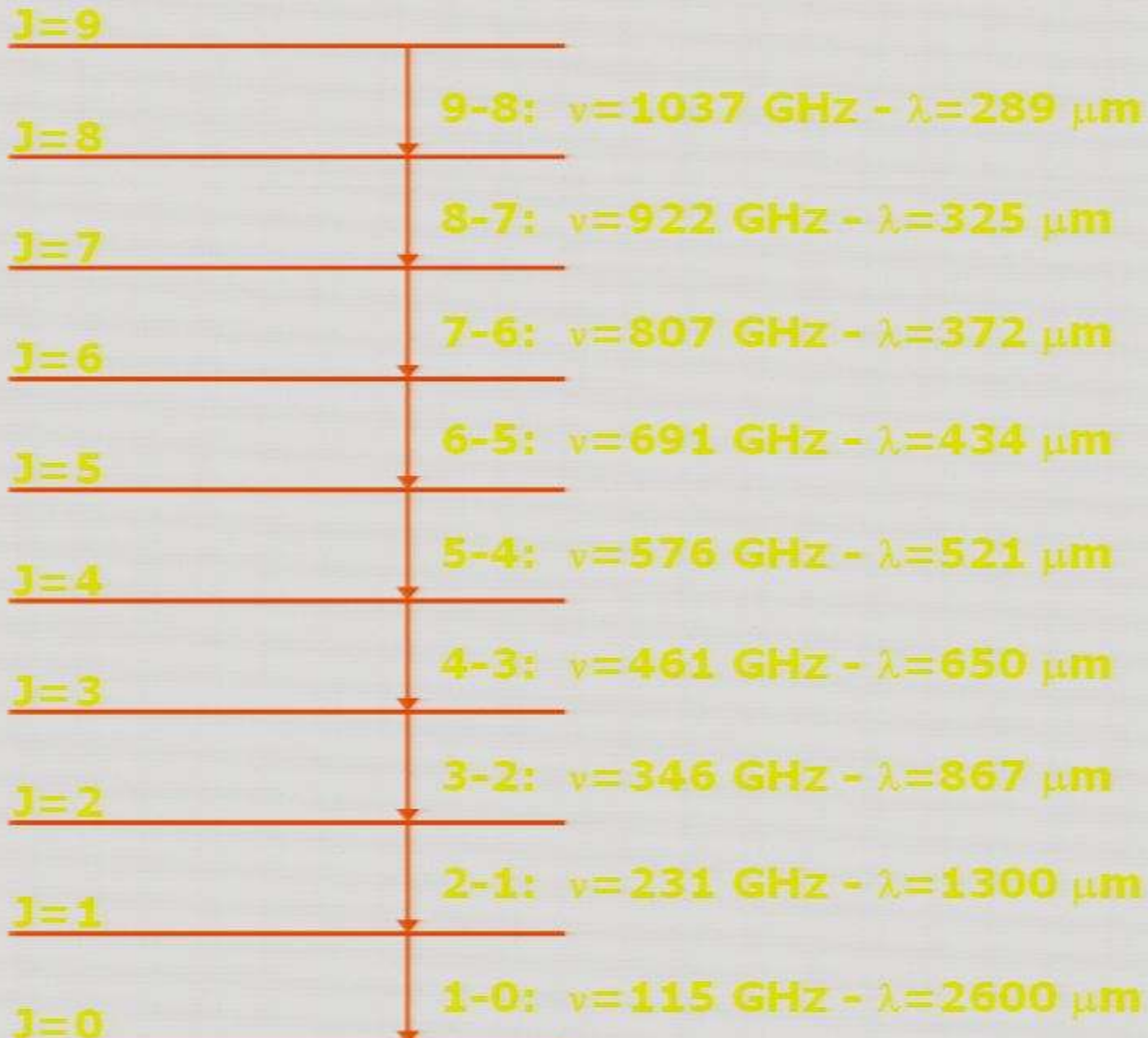
# $^{57}\text{Fe}$ XXIV line: clusters of galaxies

3.06 nm line

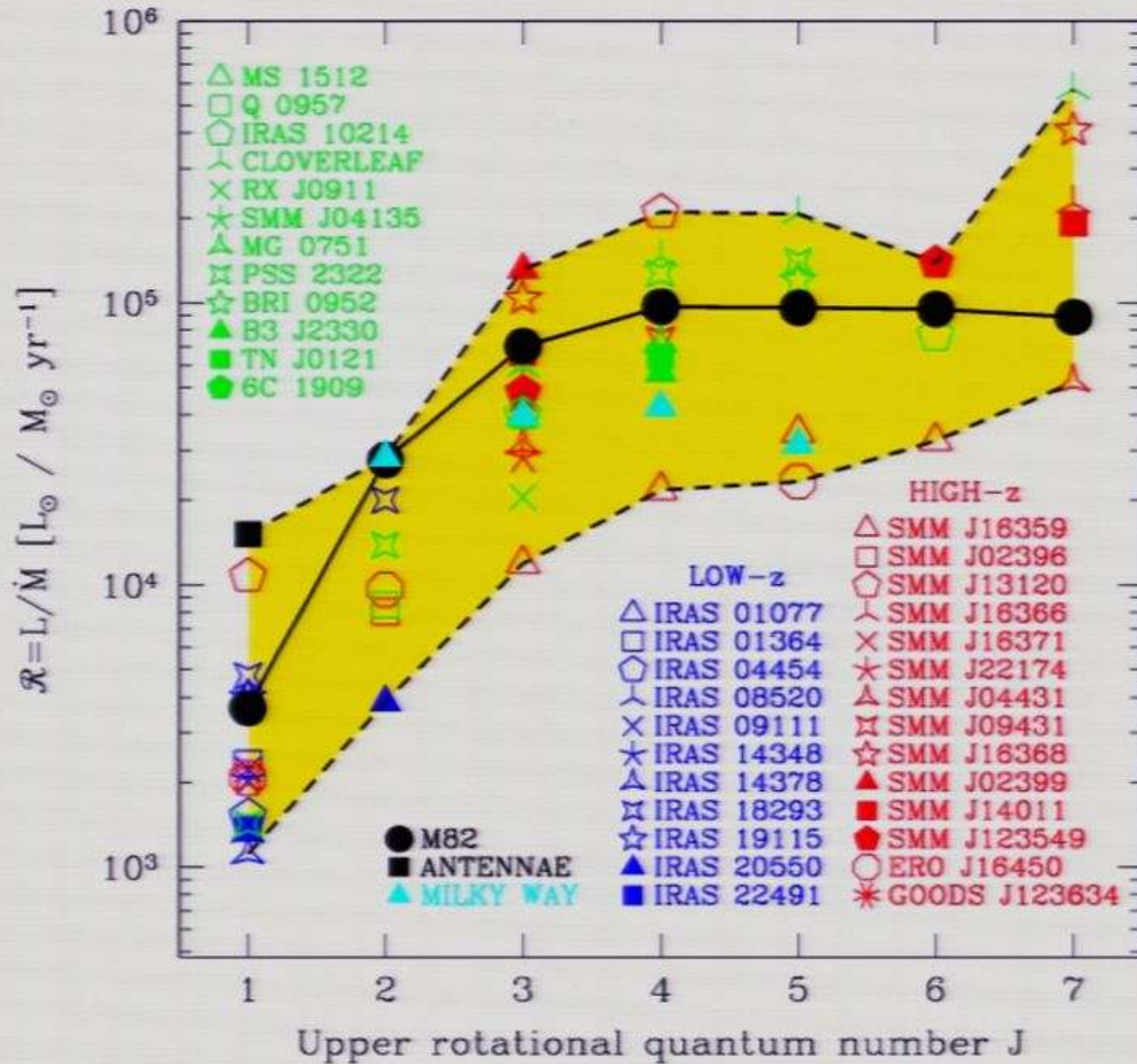
- Ion abundant at about 2 keV
- Temperature in intracluster medium
  - Central temperature decrement



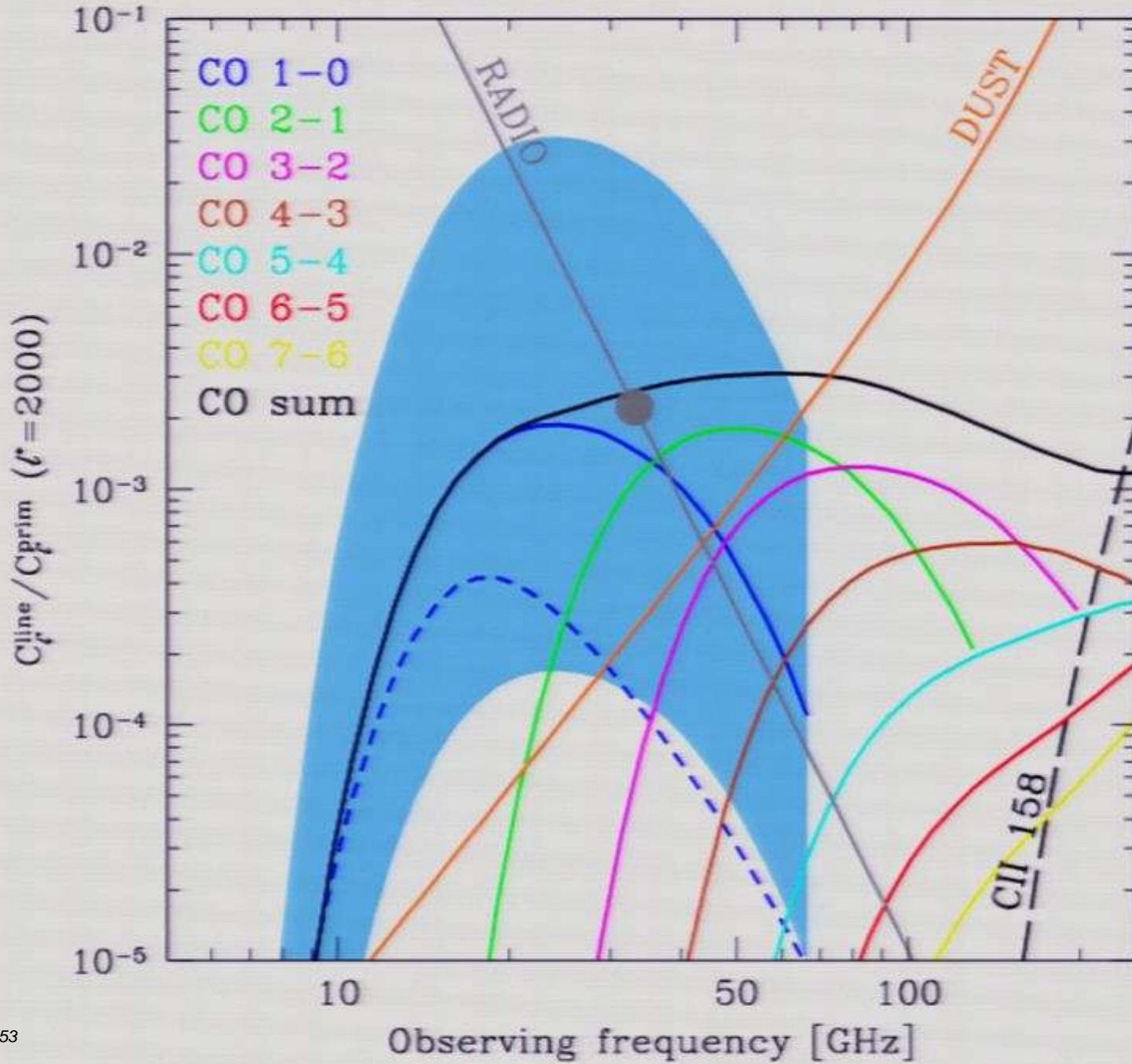
# CO rotational levels



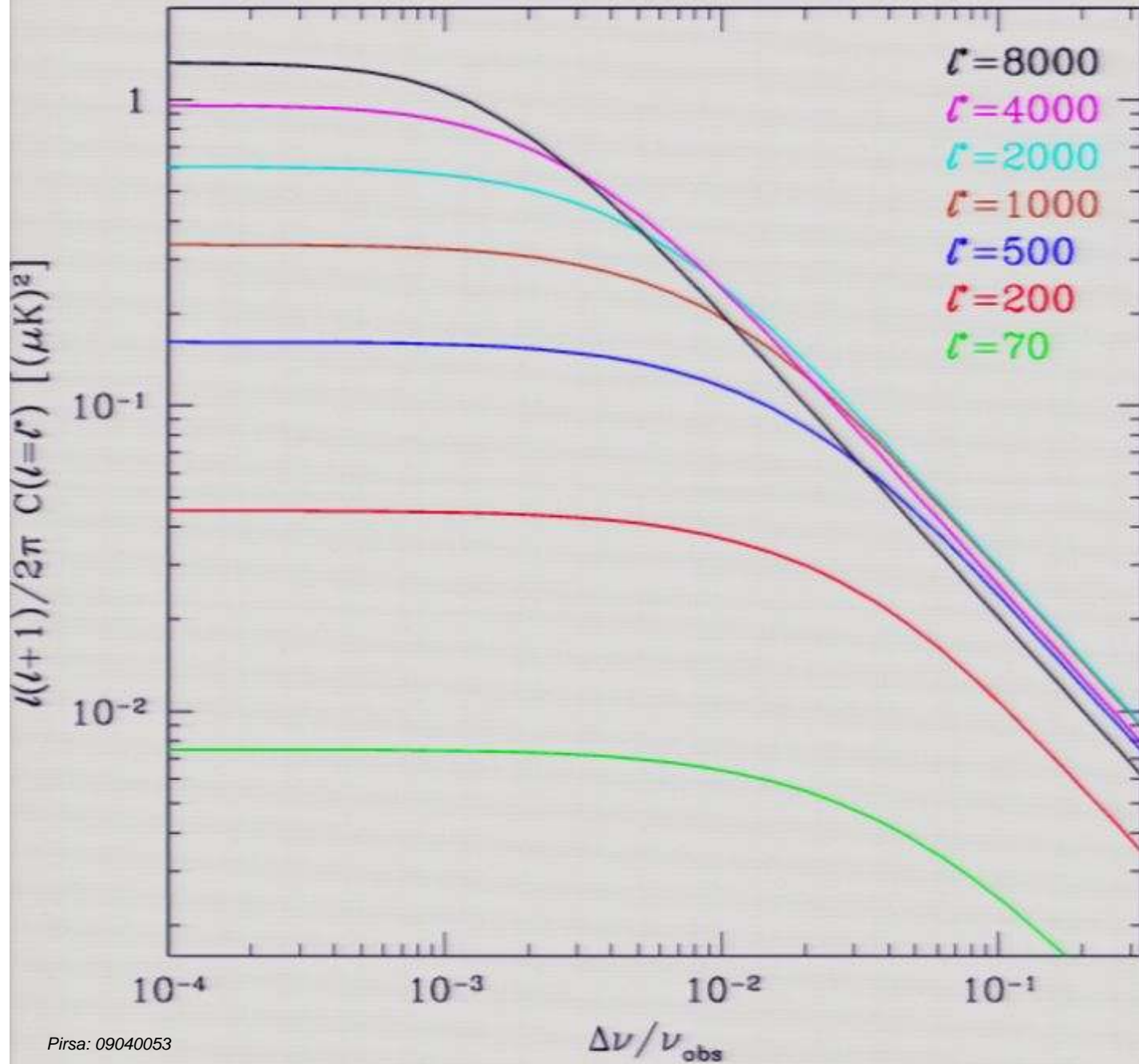
### Distribution of $\mathcal{R}$ ratios – CO lines

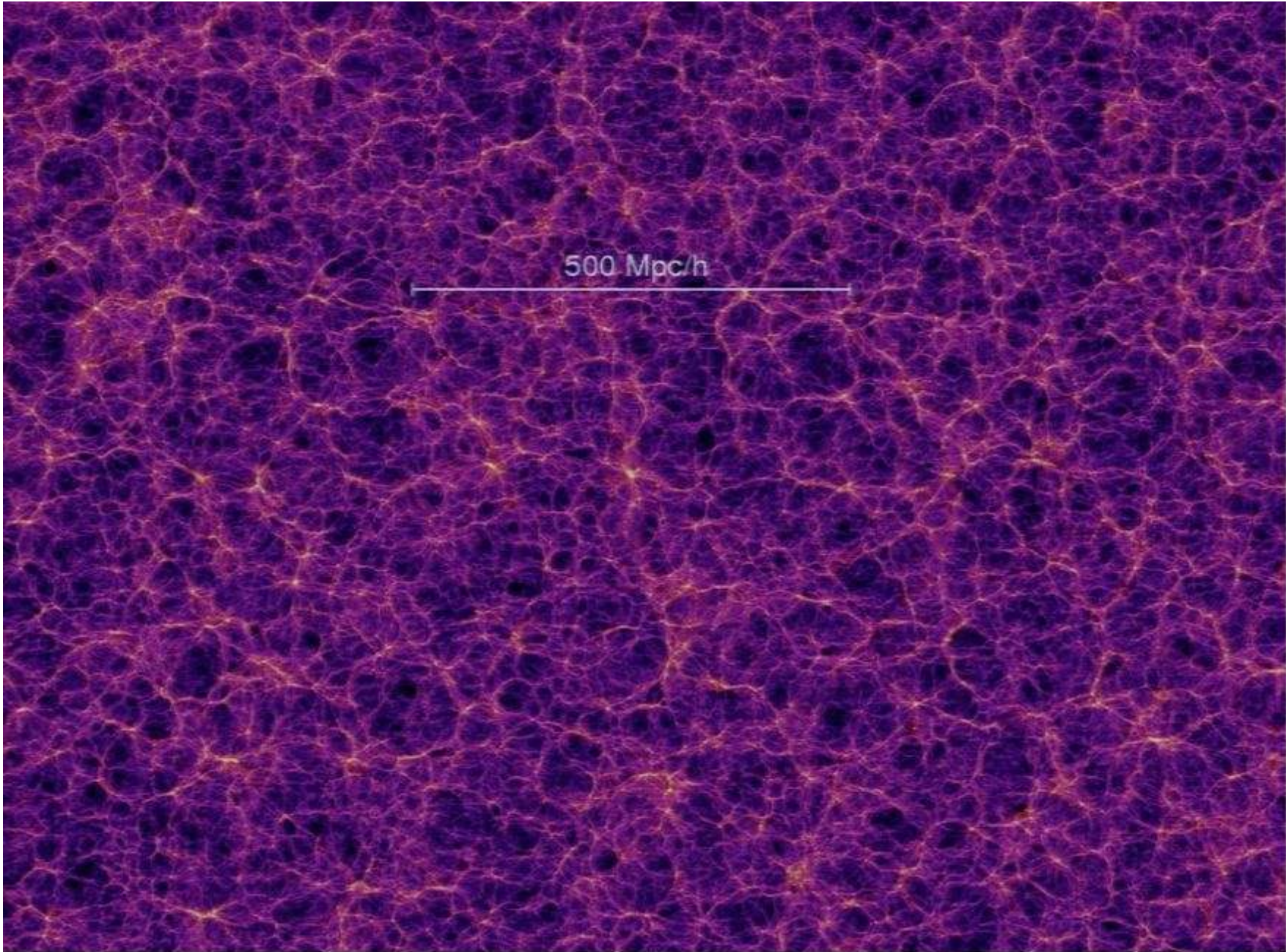


Frequency dependence -  $\Delta\nu/\nu_{\text{obs}} = 10^{-3}$

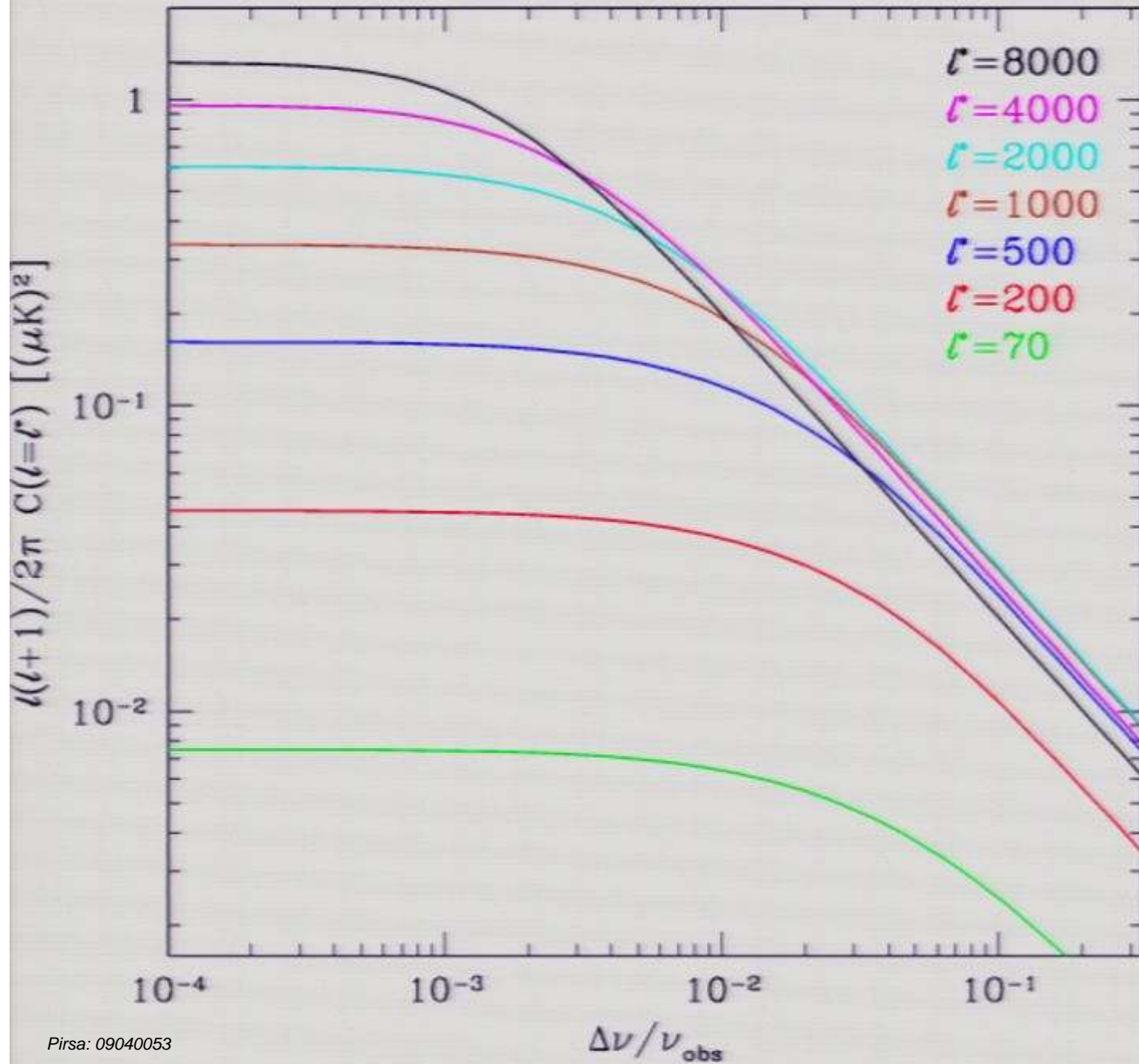


# Spectral resolution - CO 1-0 line - 30 GHz

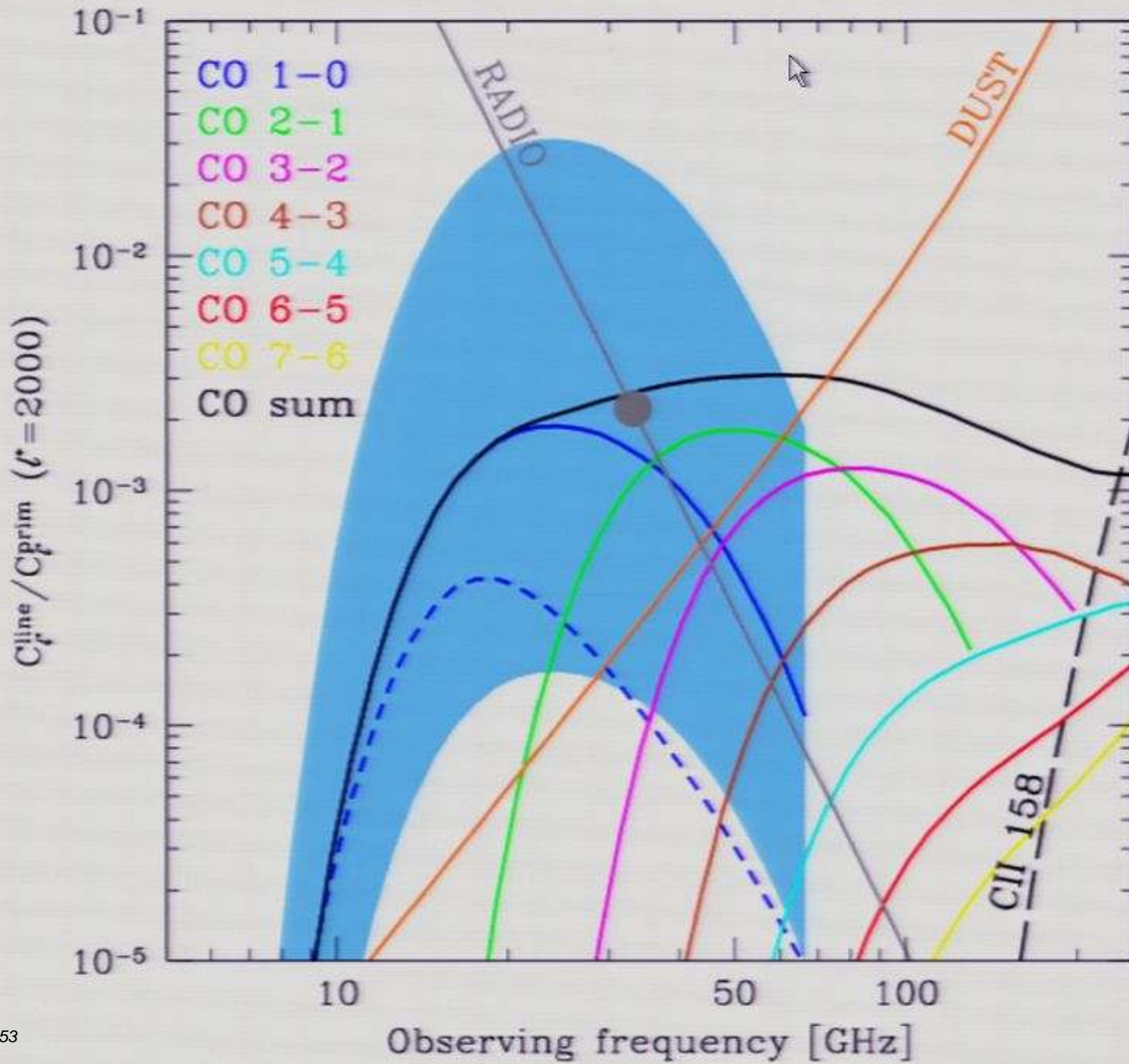




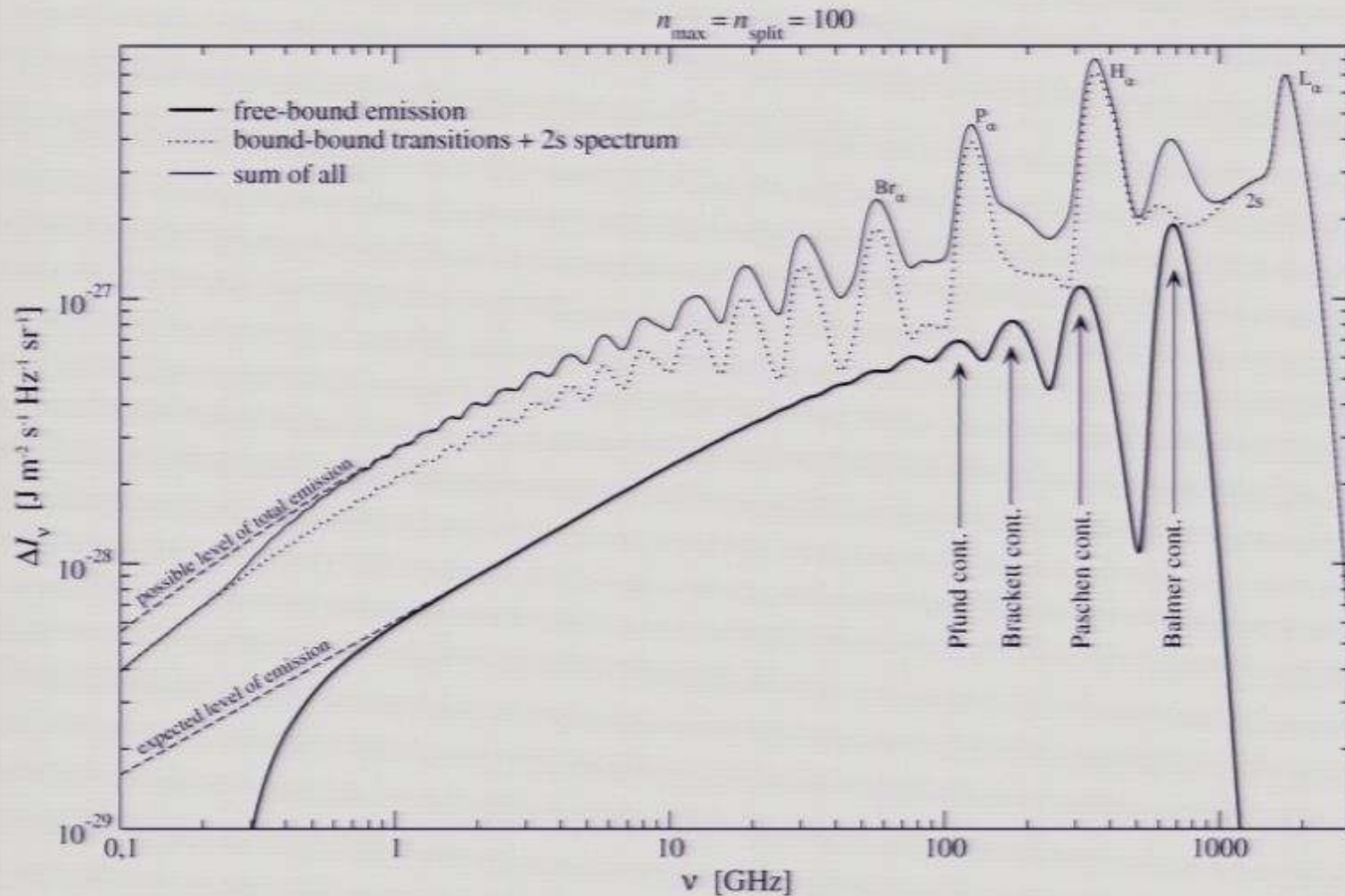
Spectral resolution – CO 1–0 line – 30 GHz



Frequency dependence -  $\Delta\nu/\nu_{\text{obs}} = 10^{-3}$



# 100-shell hydrogen atom and continuum CMB spectral distortions



## bound-bound & 2s:

- at  $\nu > 1$  GHz: distinct features
- slope  $\sim 0.46$

## free-bound:

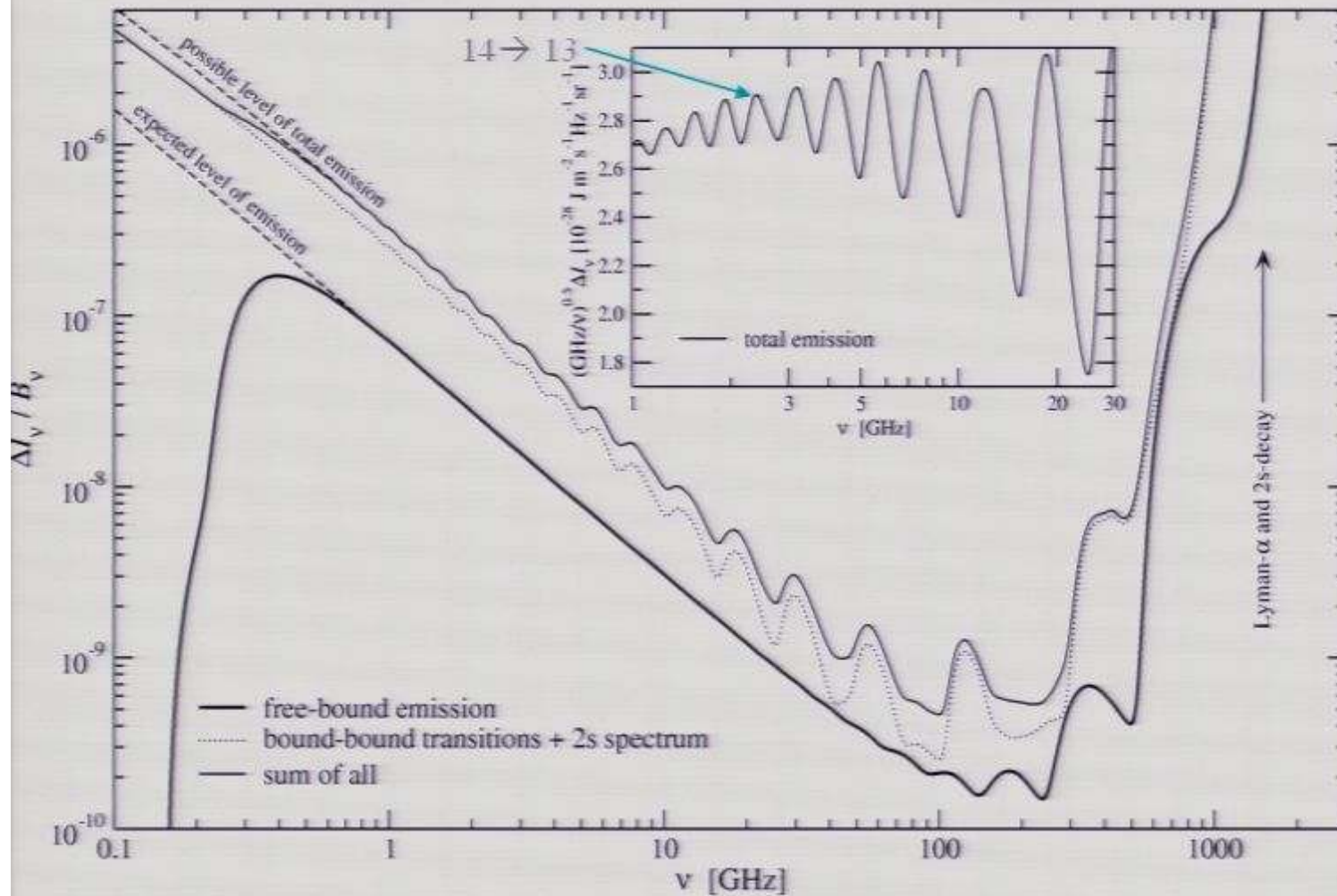
- only a few features distinguishable
- slope  $\sim 0.6$

## Total:

- f-b contributes  $\sim 30\%$  and more
- Balmer cont.  $\sim 90\%$
- Balmer:  $1\gamma$  per HI
- in total  $5\gamma$  per HI

# 100-shell hydrogen atom and continuum

## Relative distortions



### Wien-region:

- $L_\alpha$  and 2s distortions are very strong
- but CIB more dominant

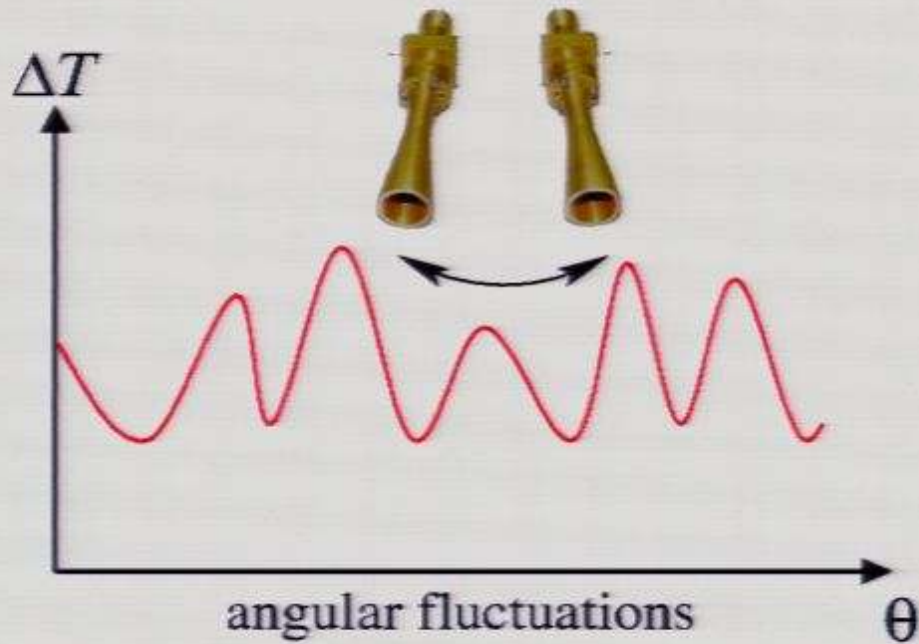
### @ CMB maximum:

- relative distortions extremely small
- strong  $\nu$ -dependence

### RJ-region:

- relative distortion exceeds level of  $\sim 10^{-7}$  below  $\nu \sim 1$ -2 GHz
- oscillatory frequency dependence with  $\sim 10$  percent-level amplitude:

*hard to mimic by known foregrounds*



**Scan over frequency  
instead of angular  
coordinate!!!**

